

Test-Agnostic Long-Tailed Recognition by Test-Time Aggregating Diverse Experts with Self-Supervision

Yifan Zhang¹ Bryan Hooi¹ Lanqing Hong² Jiashi Feng¹

¹National University of Singapore ²Huawei Noah's Ark Lab

yifan.zhang@u.nus.edu, jshfeng@gmail.com

Abstract

Existing long-tailed recognition methods, aiming to train class-balanced models from long-tailed data, generally assume the models would be evaluated on the uniform test class distribution. However, practical test class distributions often violate this assumption (e.g., being long-tailed or even inversely long-tailed), which would lead existing methods to fail in real-world applications. In this work, we study a more practical task setting, called **test-agnostic long-tailed recognition**, where the training class distribution is long-tailed while the test class distribution is unknown and can be skewed arbitrarily. In addition to the issue of class imbalance, this task poses another challenge: the class distribution shift between the training and test samples is unidentified. To handle this task, we propose a new method, called **Test-time Aggregating Diverse Experts**, that presents two solution strategies: (1) a new skill-diverse expert learning strategy that trains diverse experts to excel at handling different class distributions from a single long-tailed training distribution; (2) a novel test-time expert aggregation strategy that leverages self-supervision to aggregate multiple experts for handling various unknown test distributions. We theoretically show that our method has a provable ability to simulate the test class distribution. Extensive experiments verify that our method achieves new state-of-the-art performance on both vanilla and test-agnostic long-tailed recognition, where only three experts are sufficient to handle arbitrarily varied test class distributions. Code is available at <https://github.com/Vanint/TADE-AgnosticLT>.

1. Introduction

Real-world visual recognition problems typically exhibit a long-tailed training class distribution, where a few classes contain plenty of samples but the others are associated with only a few samples [25, 30]. Due to the imbalance of training data numbers among classes, the trained model can be easily biased towards head classes and performs poorly on tail classes [2, 51]. To deal with this, plenty of studies have been conducted to explore long-tailed recognition [10, 22, 48].

Most existing long-tailed methods [3, 10, 12] assume the test class distribution is uniform, i.e., each class has an equal number of test samples. Driven by this assumption, those methods develop various techniques, e.g., re-sampling [15, 21, 26, 47], cost-sensitive learning [13, 23, 32, 34, 39] or ensemble learning [2, 15, 27, 45, 56], to balance the model performance on different classes. However, this assumption does not always hold in real-world applications [20]. Instead, actual test samples may follow any kind of class distribution, being either uniform, long-tailed as the training data, or even inversely long-tailed to the training data, as shown in Figure 1(a). In such cases, existing methods may perform poorly, especially in the inversely long-tailed cases.

To investigate the generalization limitation of existing methods under these practical settings, we evaluate their performance on ImageNet-LT with various test class distributions. The results in Table 1 show that the models trained by existing methods suffer from a *simulation bias*, i.e., their predictions strive to simulate a specific preset class distribution. For example, the model trained with the regular softmax loss simulates the long-tailed training distribution, while the models obtained from existing long-tailed methods try to simulate the uniform class distribution. More critically, when the actual test class distribution deviates from the assumed uniform one, the simulation bias of existing long-tailed methods still exists and does not adapt, leading the resulting models to generalize poorly.

Motivated by the above observation, we consider a more practical task, namely *test-agnostic long-tailed recognition*, where the training class distribution is long-tailed while the test class distribution is arbitrary and unknown. To handle this task, we further explore the simulation property of existing methods (c.f. Table 1) that the models learned by various approaches excel at handling test class distributions with different skewness. Inspired by this, we propose to learn multiple skill-diverse experts from a single long-tailed training class distribution, as shown in Figure 1(b). Such a multi-expert model can deal with arbitrary test class distributions, as long as these skill-diverse experts are aggregated suitably at test time.

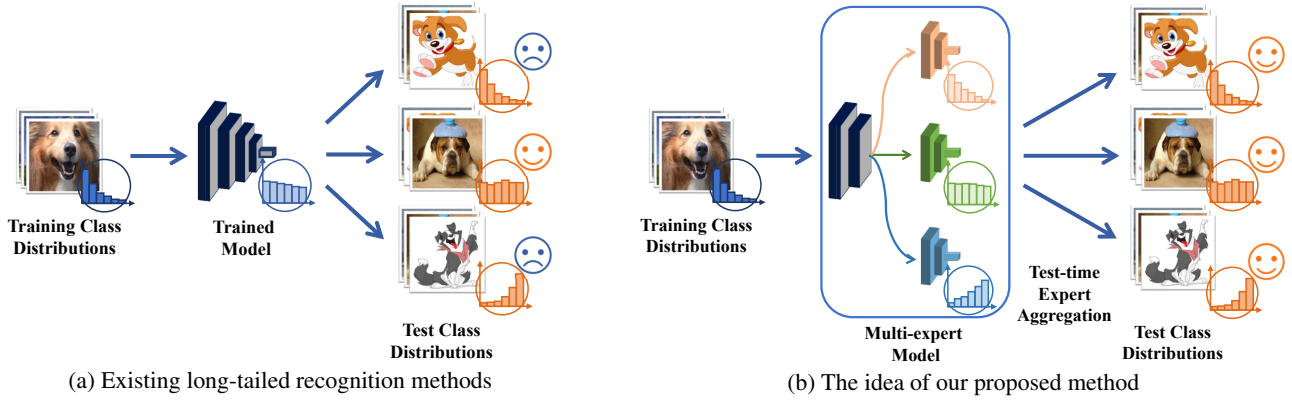


Figure 1. Illustration of test-agnostic long-tailed recognition. (a) Existing long-tailed recognition methods aim to train models that perform well on the test data with the uniform class distribution. However, the resulting models may fail to handle practical test class distributions that skew arbitrarily. (b) Our method seeks to learn a multi-expert model, where different experts are skilled in handling different class distributions. By reasonably aggregating these experts at test time, our method is able to handle any unknown test class distributions.

Following the above idea, we propose a novel method, namely Test-time Aggregating Diverse Experts (TADE), with two solution strategies: skill-diverse expert learning and test-time self-supervised aggregation. Specifically, TADE innovates the multi-expert scheme by training different experts to handle different class distributions (c.f. Figure 1(b)) via diversity-promoting expertise-guided losses. Here, various expertise-guided losses train experts to be good at handling various class distributions. As a result, the learned experts are more diverse than existing multi-expert methods [41, 56], leading to better ensemble performance, and, in aggregate, simulating a wide spectrum of possible class distributions. Then, TADE applies a new self-supervised method, namely prediction stability maximization, to adaptively aggregate experts based on unlabeled test data for handling the unknown test distribution. We theoretically show that maximizing the prediction stability (*i.e.*, prediction similarity between a sample’s two perturbed views) enables TADE to learn an aggregation weight that maximizes the mutual information between the predicted label distribution and the true class distribution. In this way, the resulting model is able to simulate arbitrary unknown test class distributions.

We empirically demonstrate TADE on both vanilla and test-agnostic long-tailed recognition. Specifically, TADE achieves new state-of-the-art performance on vanilla long-tailed recognition under all benchmark datasets. For instance, TADE achieves 58.8% accuracy on ImageNet-LT with more than 2% performance gain compared to the current state-of-the-art RIDE [41] and ACE [2]. More importantly, TADE is the first method being able to handle various test class distributions without using any test prior knowledge. Note that TADE even outperforms the model that uses the prior knowledge of test class distributions.

We make the following contributions in this work.

- To the best of our knowledge, we are among the first to study test-agnostic long-tailed recognition, without using any prior knowledge of test class distributions.

- To handle this challenging task, we present a novel TADE method. We theoretically show its provable ability to simulate unknown test class distributions, and also empirically verify its state-of-the-art performance on both vanilla and test-agnostic long-tailed recognition.

2. Related Work

Long-tailed recognition Long-tailed recognition aims to train models on highly class-imbalanced data [17, 40, 44]. Existing long-tailed methods, related to our paper, can be categorized into three classes: class re-balancing, logit adjustment and ensemble learning. Class re-balancing resorts to re-sampling [4, 15, 21, 26] or cost-sensitive learning [3, 12, 53, 54] to balance different classes during model training. Logit adjustment [20, 30, 36] adjusts the output logits of models based on the label frequencies of training data at inference time, so that a large relative margin between head and tail classes is obtained. Ensemble-based methods [2, 15, 45, 56], *e.g.*, RIDE [41], are based on multiple experts, which seek to capture heterogeneous knowledge, followed by ensemble aggregation. More discussions on the difference between our method and RIDE [41] can be found in Appendix D.1. Regarding test-agnostic long-tailed recognition, a very recent study (LADE) [20] assumes the prior of test class distributions is available and uses the test prior to post-adjust model predictions. In contrast, our method seeks to handle this problem without using any test distribution prior.

Test-time learning Test-time learning [24, 33] was proposed to handle distribution shift between training and test data [29, 49, 52], and has been applied with success to out-of-domain generalization [31, 38] and dynamic scene de-blurring [7]. In this paper, we explore this paradigm to handle test-agnostic long-tailed recognition by developing a new self-supervised learning strategy. Note that most existing self-supervised studies [5, 18, 25] focus on model pre-training [50], but few have explored test-time learning.

3. Problem Formulation

Long-tailed recognition aims to learn a classification model from a training dataset with long-tailed class distribution. Let $\mathcal{D}_s = \{x_i, y_i\}_{i=1}^{n_s}$ denote the long-tailed training dataset, where y_i is the class label of the sample x_i . The total number of training samples over C classes is $n_s = \sum_{k=1}^C n_k$, where n_k denotes the number of samples in class k . Without loss of generality, we follow a common assumption [20, 26] that the classes are sorted by cardinality in decreasing order (i.e., if $i_1 < i_2$, then $n_{i_1} \geq n_{i_2}$), and $n_1 \gg n_C$. The imbalance ratio is defined as $\max(n_k)/\min(n_k) = n_1/n_C$. The test data $\mathcal{D}_t = \{x_j, y_j\}_{j=1}^{n_t}$ is defined in a similar way.

Most existing long-tailed recognition methods assume the test class distribution is uniform (i.e., $p_t(y) = 1/C$), and seek to train models from the long-tailed training distribution $p_s(y)$ that perform well on the uniform test distribution. However, such an assumption does not always hold in practice. The actual test class distribution in real-world applications may also be long-tailed (i.e., $p_t(y) = p_s(y)$), or even inversely long-tailed to the training data (i.e., $p_t(y) = \text{inv}(p_s(y))$). Here, $\text{inv}(\cdot)$ indicates that the order of the long tail on classes is flipped. As a result, the models learned by existing methods may fail when the actual test class distribution is different from the assumed one.

To address this, we seek to study a more practical long-tailed recognition problem, i.e., **Test-agnostic Long-tailed Recognition**. This task aims to learn a recognition model from long-tailed training data, where the resulting model will be evaluated on multiple test sets that follow different class distributions. This task is difficult due to the integration of two challenges: (1) severe class imbalance in the training data makes model learning difficult; (2) unknown class distribution shift between training and test data (i.e., $p_t(y) \neq p_s(y)$) makes the model hard to generalize. To handle this task, we propose a novel method, namely Test-time Aggregating Diverse Experts.

4. Method

4.1. Motivation and Method Overview

We first analyze why existing long-tailed methods cannot handle test-agnostic long-tailed recognition, followed by elaborating on the overall scheme of our method.

Observation We evaluate some representative long-tailed methods [20, 23, 26, 41, 55] on various test class distributions, including the uniform, forward long-tailed and backward long-tailed ones. The results are given in Table 1, where the “Forward-LT- N ” and “Backward-LT- N ” indicate the cases where test samples follow the same long-tailed distribution as training data and the inversely long-tailed distribution to the training data, with the imbalance ratio N , respectively. Here, the imbalance ratio is defined in Section 3.

Test Dist.	Softmax			Decouple-LWS [26]			Balanced Softmax [23]		
	Many	Med.	Few	Many	Med.	Few	Many	Med.	Few
Forward-LT-50	67.5	41.7	14.0	61.2	49.5	27.9	63.5	47.8	37.5
Forward-LT-10	68.2	40.9	14.0	61.6	47.5	29.3	64.1	48.2	31.2
Uniform	68.1	41.5	14.0	61.8	47.6	30.9	64.1	48.2	33.4
Backward-LT-10	67.4	41.9	13.9	60.8	48.4	31.1	63.4	49.1	33.6
Backward-LT-50	70.9	41.1	13.8	66.2	44.9	30.9	66.5	48.4	33.2

Test Dist.	MiSLAS [55]			LADE w/o prior [20]			RIDE [41]		
	Many	Med.	Few	Many	Med.	Few	Many	Med.	Few
Forward-LT-50	61.6	50.0	33.3	63.5	46.4	33.1	68.3	51.6	36.8
Forward-LT-10	62.1	47.8	32.5	64.7	47.1	32.2	68.9	52.9	38.5
Uniform	62.0	49.1	32.8	64.4	47.7	34.3	68.0	52.9	35.1
Backward-LT-10	61.6	49.5	32.8	64.4	48.2	34.2	68.3	53.3	36.2
Backward-LT-50	64.2	49.3	32.5	66.3	47.8	34.0	70.8	52.5	36.1

Table 1. Top-1 accuracy of existing methods on ImageNet-LT with different test class distributions, including uniform, forward and backward long-tailed ones with imbalance ratios 10 and 50, respectively. The results show that each method performs very similarly on different test class distributions in terms of many-shot, medium-shot and few-shot classes (c.f. Section 5.1 for the partition criterion of classes). Please refer to Figure 4 in Appendix for a visualization illustration.

Table 1 shows that a specific method, e.g., Softmax, performs quite similarly on the many-shot, medium-shot and few-shot class subsets even though the test class distributions change significantly. We call this issue *simulation bias*, i.e., the trained model by a method seeks to simulate a specific class distribution without adaptation. For example, the model obtained from the regular softmax loss simulates the original long-tailed training distribution, so it performs poorly on the few-shot classes even though the test class distribution is backward long-tailed. In contrast, the models trained by existing long-tailed recognition methods seek to simulate a more uniform class distribution. More critically, when the test class distribution varies, the simulation bias does not adapt and remains unchanged. As a result, despite performing well on the uniform test class distributions, existing long-tailed recognition methods cannot adapt well to other test class distributions (c.f. Table 9).

Method overview From Table 1, we further observe that the models learned by different approaches are good at dealing with test class distributions with different skewness. That is, the model trained with the softmax loss is good at the long-tailed class distribution, while the model obtained from existing long-tailed methods is expert in the uniform class distribution. To leverage their individual advantages, we propose a novel method to handle test-agnostic long-tailed recognition, namely Test-time Aggregating Diverse Experts (TADE). TADE introduces two solution strategies: (1) learning skill-diverse experts to constitute a multi-expert model from long-tailed training data; (2) test-time learning a suitable aggregation scheme for experts with self-supervision to handle arbitrary unknown test class distributions. With these two strategies, TADE is able to deal with test-agnostic class distributions, providing a better choice for model deployment in real-world long-tailed applications.

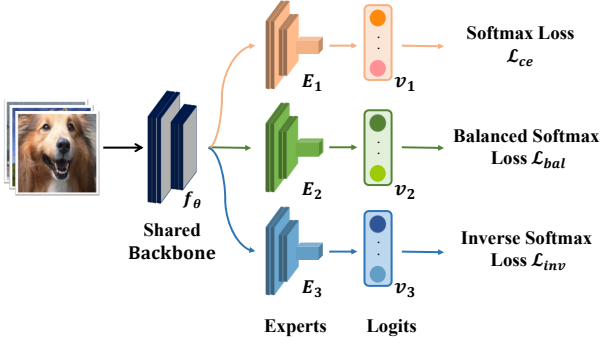


Figure 2. The scheme of TADE with three experts, where different experts are trained with different expertise-guided losses.

4.2. Skill-diverse Expert Learning

Skill-diverse multi-expert framework Existing ensemble-based long-tailed methods seek to train experts for handling the uniform test class distribution, so the trained experts are not differentiated sufficiently for handling various class distributions (refer to Table 4 for an example). To address this, TADE develops a novel skill-diverse multi-expert framework, where different experts are trained to be skilled in different class distributions and, in aggregate, span a wide spectrum of possible class distributions.

As shown in Figure 2, TADE builds a three-expert model¹ that comprises two components: (1) an expert-shared backbone f_θ ; (2) independent expert networks E_1 , E_2 and E_3 . Without loss of generality, we take ResNet [19] as an example to illustrate the multi-expert model. Since the shallow layers extract more general features and deeper layers extract more task-specific features [46], the three-expert model uses the first two stages of ResNet as the expert-shared backbone, while the later stages of ResNet and the fully-connected layer constitute independent components of each expert. The final prediction is the arithmetic mean of the prediction logits of these experts, followed by a softmax function. In order to learn skill-diverse experts, TADE trains experts with different expertise-guided objectives as follows.

Expertise-guided losses As shown in Figure 1(b), the three experts are trained to be skilled in different class distributions. The forward expert E_1 seeks to be good at the long-tailed distribution as training data and performs well on many-shot classes; the uniform expert E_2 aims to excel at the uniform distribution; the backward expert E_3 strives to be skilled in the inversely long-tailed distribution and performs well on few-shot classes. Here, the forward and backward experts are necessary since they span a wide spectrum of possible class distributions, while the uniform expert ensures that we retain high accuracy on the uniform class distribution. To this end, we use three different expertise-guided loss functions to train experts, respectively.

¹See Appendix E.1 for discussions on the number of experts and Appendix G for the model complexity.

For the **forward expert** E_1 , we directly use the softmax cross-entropy loss to train the expert so that it can simulate the original long-tailed training distribution:

$$\mathcal{L}_{ce} = \frac{1}{n_s} \sum_{x_i \in \mathcal{D}_s} -y_i \log \sigma(v_1(x_i)), \quad (1)$$

where $v_1(\cdot)$ is the output logits of the forward expert E_1 , and $\sigma(\cdot)$ is the softmax function.

For the **uniform expert** E_2 , we aim to train the expert to simulate the uniform class distribution. Inspired by the effectiveness of logit adjusted loss for long-tailed recognition [30], we resort to the balanced softmax loss [23]. To be specific, let $\hat{y}^k = p(y=k|x) = \frac{\exp(v^k)}{\sum_{c=1}^C \exp(v^c)}$ be the prediction probability. From Bayes' theorem, the prediction probability can be interpreted as $p(y=k|x) = \frac{p(x|y=k)p(y=k)}{p(x)}$. In long-tailed recognition, $p(x)$ and $p(x|y)$ are generally assumed to be consistent, while the key challenge is the class distribution shift $p_s(y) \neq p_t(y)$. For training a model to simulate the uniform distribution $p(y=k) = \frac{1}{C}$, we adjust the prediction probability by compensating the long-tailed class distribution with the prior of training label frequencies π [23]:

$$\hat{y}^k = \frac{\pi^k \exp(v^k)}{\sum_{c=1}^C \pi^c \exp(v^c)} = \frac{\exp(v^k + \log \pi^k)}{\sum_{c=1}^C \exp(v^c + \log \pi^c)}, \quad (2)$$

where $\pi^k = p_s(y=k) = \frac{n_k}{n}$ denotes the label frequency of class k . Then, given $v_2(\cdot)$ as the output logits of the uniform expert E_2 , the balanced softmax loss for E_2 is defined as:

$$\mathcal{L}_{bal} = \frac{1}{n_s} \sum_{x_i \in \mathcal{D}_s} -y_i \log \sigma(v_2(x_i) + \log \pi). \quad (3)$$

Intuitively, by adjusting logits to compensate the long-tailed distribution with prior π , this loss enables E_2 to output class-balanced predictions that simulate the uniform distribution.

For the **backward expert** E_3 , we seek to train it to simulate the inversely long-tailed class distribution. To this end, we follow the same idea of logit adjusted loss and adjust the prediction probability in the softmax loss by:

$$\hat{y}^k = \frac{\exp(v^k + \log \pi^k - \log \bar{\pi}^k)}{\sum_{c=1}^C \exp(v^c + \log \pi^c - \log \bar{\pi}^c)}, \quad (4)$$

where the inverse training prior $\bar{\pi}$ is obtained by inverting the order of training label frequencies π . We then propose a new inverse softmax loss to train the expert E_3 :

$$\mathcal{L}_{inv} = \frac{1}{n_s} \sum_{x_i \in \mathcal{D}_s} -y_i \log \sigma(v_3(x_i) + \log \pi - \lambda \log \bar{\pi}), \quad (5)$$

where $v_3(\cdot)$ denotes the output logits of E_3 and λ is a hyper-parameter. Intuitively, this loss adjusts the logits to compensate the long-tailed distribution with π , and further applies the reverse adjustment with $\bar{\pi}$. This enables E_3 to simulate the inversely long-tailed distribution well (please refer to Table 4 for empirical verification).

Model	Cosine similarity between view predictions					
	ImageNet-LT			CIFAR100-LT		
	Many	Med.	Few	Many	Med.	Few
Expert E_1	0.60	0.48	0.43	0.28	0.22	0.20
Expert E_2	0.56	0.50	0.45	0.25	0.21	0.19
Expert E_3	0.52	0.53	0.58	0.22	0.23	0.25

Table 2. Prediction stability of experts in terms of the cosine similarity between their predictions of a sample’s two views. Note that expert E_1 is good at many-shot classes and expert E_3 is skilled in few-shot classes. The results show that the experts are more stable in predicting the two views of a sample from their skilled classes. Here, the imbalance ratio of CIFAR100-LT is 100.

4.3. Test-time Self-supervised Aggregation

Based on the skill-diverse learning strategy, the three experts in TADE are skilled in different classes (c.f. Table 4). The remaining question is how to aggregate them to deal with unknown test class distributions.

A basic principle for expert aggregation is that the experts should play a bigger role in situations where they have expertise. Nevertheless, how to detect strong experts for various (unknown) test class distribution remains unknown. Our key insight is that strong experts should be more stable in predicting the samples from their skilled classes, even though these samples are perturbed. To verify this, we estimate the prediction stability of experts by comparing the cosine similarity between their predictions for a sample’s two augmented views. Here, the data views are generated by the data augmentation techniques in MoCo v2 [6]. Table 2 shows the *positive correlation between expertise and prediction stability* that stronger experts have higher prediction similarity between different views of samples from their favorable classes. Following this finding, we propose to explore the relative prediction stability to detect strong experts and weight experts for unknown test class distributions.

Prediction stability maximization We design a novel self-supervised method, namely prediction stability maximization, that learns aggregation weights for experts (with frozen parameters) by maximizing model prediction stability for unlabeled test samples. As shown in Figure 3, the method comprises three major components as follows.

Data view generation For a given sample x , we conduct two stochastic data augmentations to generate the sample’s two views, *i.e.*, x^1 and x^2 . Here, we use the same augmentation techniques as the advanced contrastive learning method, *i.e.*, MoCo v2 [6], which has been shown very effective in self-supervised learning.

Learnable aggregation weight Given the output logits of three experts $(v_1, v_2, v_3) \in \mathbb{R}^{3 \times C}$, we aggregate experts with a learnable aggregation weight $w = [w_1, w_2, w_3] \in \mathbb{R}^3$ and obtain the final softmax prediction by $\hat{y} = \sigma(w_1 \cdot v_1 + w_2 \cdot v_2 + w_3 \cdot v_3)$, where w is normalized before aggregation, *i.e.*, $w_1 + w_2 + w_3 = 1$.

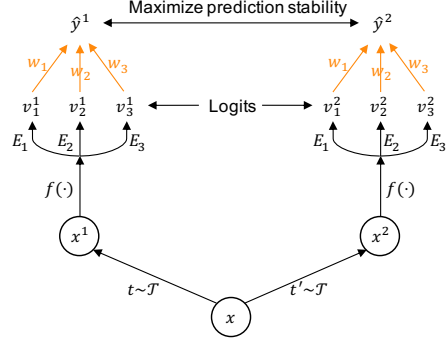


Figure 3. The scheme of test-time self-supervised aggregation. Two data augmentations sampled from the same family of augmentations ($t \sim \mathcal{T}$ and $t' \sim \mathcal{T}$) are applied to obtain two data views.

Objective function Given the view predictions of unlabeled test data, we maximize the prediction stability based on the cosine similarity between the view predictions:

$$\max_w \mathcal{S}, \text{ where } \mathcal{S} = \frac{1}{n_t} \sum_{x \in \mathcal{D}_t} \hat{y}^1 \cdot \hat{y}^2. \quad (6)$$

Here, \hat{y}^1 and \hat{y}^2 are normalized by the softmax function. In test-time training, only the aggregation weight w is updated. Since stronger experts have higher prediction similarity for their skilled classes, maximizing the prediction stability \mathcal{S} would learn higher weights for stronger experts regarding the unknown test class distribution.

4.4. Theoretical Analysis

In this section, we analyze what the prediction stability maximization strategy tends to learn. To this end, we first define the random variables of predictions and labels as $\hat{Y} \sim p(\hat{y})$ and $Y \sim p_t(y)$. We have the following result:

Theorem 1. *The prediction stability \mathcal{S} is positive proportional to the mutual information between the predicted label distribution and the test class distribution $I(\hat{Y}; Y)$, and negative proportional to the prediction entropy $H(\hat{Y})$:*

$$\mathcal{S} \propto I(\hat{Y}; Y) - H(\hat{Y}).$$

Please see Appendix A for proofs. According to Theorem 1, maximizing \mathcal{S} enables TADE to learn an aggregation weight that maximizes the mutual information between the predicted label distribution $p(\hat{y})$ and the test class distribution $p_t(y)$, as well as minimizing the prediction entropy. Since minimizing entropy improves the confidence of the classifier output [14], the aggregation weight is learned to simulate the test class distribution $p_t(y)$ and increase the prediction confidence. Such a property verifies the effectiveness of our method in test-agnostic long-tailed recognition. We provide the pseudo-code of TADE in Appendix B.

5. Experiments

We first evaluate the effectiveness of the two strategies in TADE, *i.e.*, skill-diverse expert learning and test-time self-supervised aggregation. We then evaluate the performance of TADE on vanilla and test-agnostic long-tailed recognition.

5.1. Experimental Setups

Datasets We use four benchmark datasets (*i.e.*, ImageNet-LT [28], CIFAR100-LT [3], Places-LT [28], iNaturalist 2018 [37]) to simulate real-world long-tailed data distributions. The dataset statistics are summarized in Table 3, where CIFAR100-LT has three variants with different imbalance ratios. The imbalance ratio is defined as $\max n_j / \min n_j$, where n_j denotes the data number of class $j \in [C]$.

Dataset	# classes	# training data	# test data	imbalance ratio
ImageNet-LT [28]	1,000	115,846	50,000	256
CIFAR100-LT [3]	100	50,000	10,000	{10,50,100}
Places-LT [28]	365	62,500	36,500	996
iNaturalist 2018 [37]	8,142	437,513	24,426	500

Table 3. Statistics of datasets.

Baselines We compare TADE with state-of-the-art long-tailed methods, including two-stage based methods (Decouple [26], MiSLAS [55]), logit-adjusted training (Balanced Softmax [23], LADE [20]), ensemble learning (BBN [56], ACE [2], RIDE [41]), classifier design (Causal [35]), and representation learning (PaCo [9]). Note that LADE assumes the prior of the test class distribution is accessible, while all other methods do not use any test prior.

Evaluation protocols We consider two evaluation protocols: the conventional one and the test-agnostic one. In the conventional protocol [26, 28], the models are evaluated on the uniform test class distribution in terms of top-1 accuracy. Following [28], we also report accuracy on three groups of classes: Many-shot (more than 100 images), Medium-shot (20~100 images) and Few-shot (less than 20 images). In the test-agnostic protocol, the models are evaluated on multiple sets of test samples, following different class distributions, in terms of top-1 accuracy. Following [20], we construct three kinds of test class distributions, *i.e.*, the uniform distribution, forward long-tailed distributions as training data, and backward long-tailed distributions. In the backward ones, the order of the long tail on classes is flipped. More details of test data construction can be found in Appendix C.1.

Implementation details We implement our method in PyTorch. Following [20, 41], we use ResNeXt-50 for ImageNet-LT, ResNet-32 for CIFAR100-LT, ResNet-152 for Places-LT and ResNet-50 for iNaturalist 2018 as backbones. If not specified, we use SGD optimizer with the momentum 0.9 and the learning rate 0.1 (linear decay). We set $\lambda=2$ for ImageNet-LT and CIFAR100-LT, and $\lambda=1$ for the rest datasets. In test-time training, we train the aggregation weights for 5 epochs. More details are reported in Appendix C.2.

Model	RIDE [41]							
	ImageNet-LT				CIFAR100-LT			
	Many	Med.	Few	All	Many	Med.	Few	All
Expert E_1	64.3	49.0	31.9	52.6	63.5	44.8	20.3	44.0
Expert E_2	64.7	49.4	31.2	52.8	63.1	44.7	20.2	43.8
Expert E_3	64.3	48.9	31.8	52.5	63.9	45.1	20.5	44.3
Ensemble	68.0	52.9	35.1	56.3	67.4	49.5	23.7	48.0

Model	TADE (ours)							
	ImageNet-LT				CIFAR100-LT			
	Many	Med.	Few	All	Many	Med.	Few	All
Expert E_1	68.8	43.7	17.2	49.8	67.6	36.3	6.8	38.4
Expert E_2	65.5	50.5	33.3	53.9	61.2	44.7	23.5	44.2
Expert E_3	43.4	48.6	53.9	47.3	14.0	27.6	41.2	25.8
Ensemble	67.0	56.7	42.6	58.8	61.6	50.5	33.9	49.4

Table 4. Performance of each expert on the uniform test distribution, where the imbalance ratio of CIFAR100-LT is 100. The results show that our proposed method can learn more skill-diverse experts, which lead to better performance of ensemble aggregation.

Test Dist.	Expert E_1 (w_1)	Expert E_2 (w_2)	Expert E_3 (w_3)
Forward-LT-50	0.52	0.35	0.13
Forward-LT-10	0.46	0.36	0.18
Uniform	0.33	0.33	0.34
Backward-LT-10	0.21	0.29	0.50
Backward-LT-50	0.17	0.27	0.56

Table 5. The learned aggregation weights by our test-time aggregation strategy on ImageNet-LT under various test class distributions. The results show that our method can learn suitable expert weights for various unknown test class distributions.

5.2. Effectiveness of Skill-diverse Expert Learning

This section examines the skill-diverse expert learning strategy. We report the results in Table 4, where RIDE [41] is a state-of-the-art ensemble-based method. Specifically, RIDE trains each expert with cross-entropy independently and uses KL-Divergence to improve expert diversity. However, simply maximizing the divergence of expert predictions cannot learn visibly diverse experts, as shown in Table 4. In contrast, the three experts trained by our expertise-guided losses learn very different expertise, excelling at many-shot classes, the uniform class distribution (with higher overall performance), and few-shot classes, respectively. As a result, the increasing expert diversity leads to a non-trivial gain of overall performance for TADE compared to RIDE. More results are reported in Appendix D.1.

5.3. Effectiveness of Test-time Expert Aggregation

As shown in Table 5, our test-time self-supervised aggregation method can learn suitable expert weights for various unknown test class distributions. For forward long-tailed distributions, the weight of the forward expert E_1 is higher, while for backward long-tailed distributions, the weight of the backward expert E_3 is relatively high. As a result, our method enhances the performance of the dominant test classes in arbitrary test class distributions, leading to better overall performance as shown in Table 6. Moreover, as the test dataset gets more imbalanced, the performance gain gets larger. More results are reported in Appendix D.2.

Test Dist.	ImageNet-LT							
	Ours w/o test-time aggregation				Ours w/ test-time aggregation			
	Many	Med.	Few	All	Many	Med.	Few	All
Forward-LT-50	65.6	55.7	44.1	65.5	70.0	53.2	33.1	69.4 (+3.9)
Forward-LT-10	66.5	56.8	44.2	63.6	69.9	54.3	34.7	65.4 (+1.8)
Uniform	67.0	56.7	42.6	58.8	66.5	57.0	43.5	58.8 (+0.0)
Backward-LT-10	65.0	57.6	43.1	53.1	60.9	57.5	50.1	54.5 (+1.4)
Backward-LT-50	69.1	57.0	42.9	49.8	60.7	56.2	50.7	53.1 (+3.3)

Table 6. The performance improvement via test-time self-supervised aggregation under various test class distributions on ImageNet-LT.

Method	Many	Med.	Few	All
Softmax	68.1	41.5	14.0	48.0
Decouple-LWS [26]	61.8	47.6	30.9	50.8
Causal [35]	64.1	45.8	27.2	50.3
Balanced Softmax [23]	64.1	48.2	33.4	52.3
MiSLAS [55]	62.0	49.1	32.8	51.4
LADE [20]	64.4	47.7	34.3	52.3
PaCo [9]	63.2	51.6	39.2	54.4
ACE [2]	71.7	54.6	23.5	56.6
RIDE [41]	68.0	52.9	35.1	56.3
TADE (ours)	66.5	57.0	43.5	58.8

Table 7. Top-1 accuracy on ImageNet-LT.

Imbalance Ratio	10	50	100
Softmax	59.1	45.6	41.4
BBN [56]	59.8	49.3	44.7
Causal [35]	59.4	48.8	45.0
Balanced Softmax [23]	61.0	50.9	46.1
MiSLAS [55]	62.5	51.5	46.8
LADE [20]	61.6	50.1	45.6
RIDE [41]	61.8	51.7	48.0
TADE (ours)	63.6	53.9	49.8

(a) CIFAR100-LT

Method	Top-1 accuracy
Softmax	31.4
Causal [35]	32.2
Balanced Softmax [23]	39.4
MiSLAS [55]	38.3
LADE [20]	39.2
RIDE [41]	40.3
TADE (ours)	40.9

(b) Places-LT

Method	Top-1 accuracy
Softmax	64.7
Causal [35]	64.4
Balanced Softmax [23]	70.6
MiSLAS [55]	70.7
LADE [20]	69.3
RIDE [41]	71.8
TADE (ours)	72.9

(c) iNaturalist 2018

Table 8. Top-1 accuracy on CIFAR100-LT, Places-LT and iNaturalist 2018, where the test class distribution is uniform. More results on three sub-groups of classes are reported in Appendix D.

5.4. Results on Uniform Test Class Distribution

This section compares TADE with state-of-the-art long-tailed methods under the uniform test class distribution.

ImageNet-LT We train models for 180 epochs with cosine learning rate decay. The batch size for most baselines is 256 (learning rate 0.1), while that for RIDE and our method is 64 (learning rate 0.025). As reported in Table 7, Softmax trains the model with only cross-entropy, so it simulates the long-tailed training class distribution and performs well on many-shot classes. However, it performs worse on medium-shot and few-shot classes, leading to worse overall performance. In contrast, existing long-tailed methods (*e.g.*, Decouple, Causal) seek to simulate the uniform class distribution, and thus their performance on all classes is more balanced, leading to better overall performance. However, as these methods mainly seek for balanced performance, they inevitably sacrifice the performance on many-shot classes. To address this, RIDE and ACE explore ensemble learning for long-tailed recognition and achieve better performance on tail classes without sacrificing the head-class performance. In comparison, based on the increasing expert diversity derived from skill-diverse expert learning, our method performs the best on ImageNet-LT, with more than 2% performance gain compared to RIDE and ACE. These results demonstrate the superiority of TADE over the compared methods particularly designed for the uniform test class distribution. More experiments with stronger data augmentations (*i.e.*, RandAugment [8]) are reported in Appendix D.3.

CIFAR100-LT We train all methods for 200 epochs with batch size 128. The results are reported in Table 8(a), where all long-tailed methods outperform Softmax. One interesting observation is that RIDE outperforms all other baselines significantly under the imbalance ratio 100, but it performs worse than MiSLAS under the imbalance ratio 10. This implies when the imbalance ratio of the long-tailed data is relatively low, the naive ensemble-based long-tailed methods may be less competitive than augmentation-based long-tailed methods. In contrast, using our skill-diverse expert learning strategy to increase expert diversity, TADE outperforms all the baselines on CIFAR100-LT under all imbalance ratios. This result further demonstrates the effectiveness of our method in resolving vanilla long-tailed recognition.

Places-LT Following [26, 28], we use the ResNet-152 model pre-trained on ImageNet as the backbone. The batch size is 128 and the learning rate is 0.01. The training epoch for MiSLAS is 100, and that for all other methods is 30. As shown in Table 8(b), our proposed method also achieves state-of-the-art performance on Places-LT.

iNaturalist 2018 We train most baselines for 200 epochs with batch size 256 and learning rate 0.1. For RIDE and our method, we adjust the batch size to 512 and the learning rate to 0.2. As shown in Table 8(c), the proposed method achieves new state-of-the-art performance, *i.e.*, 72.9% top-1 accuracy. Such results demonstrate that TADE handles highly-imbalanced fine-grained image data well, even though there are a very large number of classes.

		(a) ImageNet-LT										(b) CIFAR100 (IR10)											
Method	Prior	Forward-LT					Uni.	Backward-LT					Forward-LT					Uni.	Backward-LT				
		50	25	10	5	2	1	2	5	10	25	50	50	25	10	5	2	1	2	5	10	25	50
Softmax	✗	66.1	63.8	60.3	56.6	52.0	48.0	43.9	38.6	34.9	30.9	27.6	72.0	69.6	66.4	65.0	61.2	59.1	56.3	53.5	50.5	48.7	46.5
BS	✗	63.2	61.9	59.5	57.2	54.4	52.3	50.0	47.0	45.0	42.3	40.8	65.9	64.9	64.1	63.4	61.8	61.0	60.0	58.2	57.5	56.2	55.1
MiSLAS	✗	61.6	60.4	58.0	56.3	53.7	51.4	49.2	46.1	44.0	41.5	39.5	67.0	66.1	65.5	64.4	63.2	62.5	61.2	60.4	59.3	58.5	57.7
LADE	✗	63.4	62.1	59.9	57.4	54.6	52.3	49.9	46.8	44.9	42.7	40.7	67.5	65.8	65.8	64.4	62.7	61.6	60.5	58.8	58.3	57.4	57.7
LADE	✓	65.8	63.8	60.6	57.5	54.5	52.3	50.4	48.8	48.6	49.0	49.2	71.2	69.3	67.1	64.6	62.4	61.6	60.4	61.4	61.5	62.7	64.8
RIDE	✗	67.6	66.3	64.0	61.7	58.9	56.3	54.0	51.0	48.7	46.2	44.0	67.1	65.3	63.6	62.1	60.9	61.8	58.4	56.8	55.3	54.9	53.4
TADE	✗	69.4	67.4	65.4	63.0	60.6	58.8	57.1	55.5	54.5	53.7	53.1	71.2	69.4	67.6	66.3	64.4	63.6	62.9	62.4	61.7	62.1	63.0

		(c) CIFAR100 (IR50)										(d) CIFAR100 (IR100)											
Method	Prior	Forward-LT					Uni.	Backward-LT					Forward-LT					Uni.	Backward-LT				
		50	25	10	5	2	1	2	5	10	25	50	50	25	10	5	2	1	2	5	10	25	50
Softmax	✗	64.8	62.7	58.5	55.0	49.9	45.6	40.9	36.2	32.1	26.6	24.6	63.3	62.0	56.2	52.5	46.4	41.4	36.5	30.5	25.8	21.7	17.5
BS	✗	61.6	60.2	58.4	55.9	53.7	50.9	48.5	45.7	43.9	42.5	40.6	57.8	55.5	54.2	52.0	48.7	46.1	43.6	40.8	38.4	36.3	33.7
MiSLAS	✗	60.1	58.9	57.7	56.2	53.7	51.5	48.7	46.5	44.3	41.8	40.2	58.8	57.2	55.2	53.0	49.6	46.8	43.6	40.1	37.7	33.9	32.1
LADE	✗	61.3	60.2	56.9	54.3	52.3	50.1	47.8	45.7	44.0	41.8	40.5	56.0	55.5	52.8	51.0	48.0	45.6	43.2	40.0	38.3	35.5	34.0
LADE	✓	65.9	62.1	58.8	56.0	52.3	50.1	48.3	45.5	46.5	46.8	47.8	62.6	60.2	55.6	52.7	48.2	45.6	43.8	41.1	41.5	40.7	41.6
RIDE	✗	62.2	61.0	58.8	56.4	52.9	51.7	47.1	44.0	41.4	38.7	37.1	63.0	59.9	57.0	53.6	49.4	48.0	42.5	38.1	35.4	31.6	29.2
TADE	✗	67.2	64.5	61.2	58.6	55.4	53.9	51.9	50.9	51.0	51.7	52.8	65.9	62.5	58.3	54.8	51.1	49.8	46.2	44.7	43.9	42.5	42.4

		(e) Places-LT										(f) iNaturalist 2018											
Method	Prior	Forward-LT					Uni.	Backward-LT					Forward-LT					Uni.	Backward-LT				
		50	25	10	5	2	1	2	5	10	25	50	3	2	1	2	3						
Softmax	✗	45.6	42.7	40.2	38.0	34.1	31.4	28.4	25.4	23.4	20.8	19.4	65.4	65.5	64.7	64.0	63.4						
BS	✗	42.7	41.7	41.3	41.0	40.0	39.4	38.5	37.8	37.1	36.2	35.6	70.3	70.5	70.6	70.6	70.8						
MiSLAS	✗	40.9	39.7	39.5	39.6	38.8	38.3	37.3	36.7	35.8	34.7	34.4	70.8	70.8	70.7	70.7	70.2						
LADE	✗	42.8	41.5	41.2	40.8	39.8	39.2	38.1	37.6	36.9	36.0	35.7	68.4	69.0	69.3	69.6	69.5						
LADE	✓	46.3	44.2	42.2	41.2	39.7	39.4	39.2	39.9	40.9	42.4	43.0	✗	69.1	69.3	70.2	✗						
RIDE	✗	43.1	41.8	41.6	42.0	41.0	40.3	39.6	38.7	38.2	37.0	36.9	71.5	71.9	71.8	71.9	71.8						
TADE	✗	46.4	44.9	43.3	42.6	41.3	40.9	40.6	41.1	41.4	42.0	41.6	72.3	72.5	72.9	73.5	73.3						

Table 9. Top-1 accuracy over all classes under various unknown test class distributions. “Prior” indicates that the test class distribution is used as prior knowledge. “Uni.” denotes the uniform distribution. “IR” indicates the imbalance ratio. “BS” denotes the balanced softmax [23].

5.5. Results on Test-agnostic Class Distributions

This section further compares TADE with state-of-the-art long-tailed methods under various test class distributions. More ablation studies are reported in Appendices D.4 and F.

ImageNet-LT The results on ImageNet-LT are reported in Table 9(a). Since Softmax seeks to simulate the long-tailed training distribution, it performs well on forward long-tailed test distributions. However, its performance on the uniform and backward long-tailed distributions is poor. In contrast, existing long-tailed methods show more balanced performance among classes, leading to better overall accuracy. However, the resulting models by these methods suffer from a simulation bias, *i.e.*, performing similarly among classes on various class distributions (c.f. Table 1). As a result, they cannot adapt to diverse test class distributions well.

To handle this task, LADE assumes the prior knowledge of test class distributions is available, and uses the additional prior to adjust its predictions, leading to better performance on various class distributions. However, considering that it is difficult to obtain the test prior in real-world applications, the methods that require the prior knowledge may be hard to apply in practice. In contrast, our proposed TADE applies a new self-supervised strategy to deal with unknown class distributions (c.f. Table 6), and obtains even better performance without using any test prior (c.f. Table 9(a)). The promising results demonstrate the effectiveness and practicality of our method. Note that the performance advantages of TADE become larger as the test dataset gets more imbalanced.

CIFAR100-LT and Places-LT As shown in Table 9(b-e), most observations are similar to ImageNet-LT. One interesting result is that when the backward long-tailed distribution is very imbalanced, LADE with the test prior performs the best on CIFAR100-LT (IR10) and Places-LT. In contrast, TADE performs comparably on these distributions without using any test prior.

iNaturalist 2018 Since the number of original test samples is only 3 on each class in iNaturalist 2018, the number of the constructed test class distributions is less than other datasets (c.f. Table 9(f)). Note that on Forward-LT-3 and Backward-LT-3 distributions, the number of test samples on some classes becomes zero. In such cases, the test prior cannot be used in LADE, since adjusting logits with $\log 0$ results in biased predictions. As shown in Table 9(f), TADE still performs the best on all test class distributions.

6. Conclusion

This work studies a new task of test-agnostic long-tailed recognition, where the test class distribution is unknown and arbitrary. To handle this task, we propose a novel method, namely Test-time Aggregating Diverse Experts (TADE), which consists of two new strategies, *i.e.*, skill-diverse expert learning and test-time self-supervised aggregation. We theoretically analyze our method and also empirically show that TADE achieves new state-of-the-art performance on both vanilla and test-agnostic long-tailed recognition.

References

- [1] Malik Boudiaf, Jérôme Rony, et al. A unifying mutual information view of metric learning: cross-entropy vs. pairwise losses. In *European Conference on Computer Vision*, 2020. 11
- [2] Jiarui Cai, Yizhou Wang, and Jenq-Neng Hwang. Ace: Ally complementary experts for solving long-tailed recognition in one-shot. In *International Conference on Computer Vision*, 2021. 1, 2, 6, 7
- [3] Kaidi Cao, Colin Wei, Adrien Gaidon, Nikos Arachia, and Tengyu Ma. Learning imbalanced datasets with label-distribution-aware margin loss. In *Advances in Neural Information Processing Systems*, 2019. 1, 2, 6
- [4] Nitesh V Chawla, Kevin W Bowyer, et al. Smote: synthetic minority over-sampling technique. *Journal of Artificial Intelligence Research*, 2002. 2
- [5] Ting Chen, Simon Kornblith, Mohammad Norouzi, and Geoffrey Hinton. A simple framework for contrastive learning of visual representations. In *International Conference on Machine Learning*, 2020. 2
- [6] Xinlei Chen, Haoqi Fan, Ross Girshick, and Kaiming He. Improved baselines with momentum contrastive learning. *ArXiv*, 2020. 5, 12
- [7] Zhixiang Chi, Yang Wang, et al. Test-time fast adaptation for dynamic scene deblurring via meta-auxiliary learning. In *Computer Vision and Pattern Recognition*, 2021. 2
- [8] Ekin Dogus Cubuk, Barret Zoph, Jon Shlens, and Quoc Le. Randaugment: Practical automated data augmentation with a reduced search space. In *Advances in Neural Information Processing Systems*, volume 33, 2020. 7, 16
- [9] Jiequan Cui, Zhisheng Zhong, Shu Liu, Bei Yu, and Jiaya Jia. Parametric contrastive learning. In *International Conference on Computer Vision*, 2021. 6, 7, 16
- [10] Yin Cui, Menglin Jia, et al. Class-balanced loss based on effective number of samples. In *Computer Vision and Pattern Recognition*, 2019. 1
- [11] Jia Deng, Wei Dong, Richard Socher, Li-Jia Li, Kai Li, and Li Fei-Fei. Imagenet: A large-scale hierarchical image database. In *Computer Vision and Pattern Recognition*, 2009. 12
- [12] Zongyong Deng, Hao Liu, Yaoxing Wang, Chenyang Wang, Zekuan Yu, and Xuehong Sun. Pml: Progressive margin loss for long-tailed age classification. In *Computer Vision and Pattern Recognition*, pages 10503–10512, 2021. 1, 2
- [13] Chengjian Feng, Yujie Zhong, and Weilin Huang. Exploring classification equilibrium in long-tailed object detection. In *International Conference on Computer Vision*, 2021. 1
- [14] Yves Grandvalet, Yoshua Bengio, et al. Semi-supervised learning by entropy minimization. In *CAP*, 2005. 5
- [15] Hao Guo and Song Wang. Long-tailed multi-label visual recognition by collaborative training on uniform and re-balanced samplings. In *Computer Vision and Pattern Recognition*, 2021. 1, 2
- [16] Marton Havasi, Rodolphe Jenatton, et al. Training independent subnetworks for robust prediction. In *International Conference on Learning Representations*, 2021. 24
- [17] Haibo He and Eduardo A Garcia. Learning from imbalanced data. *IEEE Transactions on Knowledge and Data Engineering*, 21(9):1263–1284, 2009. 2
- [18] Kaiming He, Haoqi Fan, Yuxin Wu, Saining Xie, and Ross Girshick. Momentum contrast for unsupervised visual representation learning. In *Computer Vision and Pattern Recognition*, 2020. 2
- [19] Kaiming He, Xiangyu Zhang, Shaoqing Ren, and Jian Sun. Deep residual learning for image recognition. In *Computer Vision and Pattern Recognition*, pages 770–778, 2016. 4
- [20] Youngkyu Hong, Seungju Han, Kwanghee Choi, Seokjun Seo, Beomsu Kim, and Buru Chang. Disentangling label distribution for long-tailed visual recognition. In *Computer Vision and Pattern Recognition*, 2021. 1, 2, 3, 6, 7, 12, 16, 17
- [21] Chen Huang, Yining Li, Chen Change Loy, and Xiaoou Tang. Learning deep representation for imbalanced classification. In *Computer Vision and Pattern Recognition*, 2016. 1, 2
- [22] Muhammad Abdullah Jamal, Matthew Brown, Ming-Hsuan Yang, Liqiang Wang, and Boqing Gong. Rethinking class-balanced methods for long-tailed visual recognition from a domain adaptation perspective. In *Computer Vision and Pattern Recognition*, pages 7610–7619, 2020. 1
- [23] Ren Jiawei, Cunjun Yu, Xiao Ma, Haiyu Zhao, Shuai Yi, et al. Balanced meta-softmax for long-tailed visual recognition. In *Advances in Neural Information Processing Systems*, 2020. 1, 3, 4, 6, 7, 8, 16, 17
- [24] Mohammad Mahdi Kamani, Sadegh Farhang, Mehrdad Mahdavi, and James Z Wang. Targeted data-driven regularization for out-of-distribution generalization. In *ACM SIGKDD International Conference on Knowledge Discovery & Data Mining*, pages 882–891, 2020. 2
- [25] Bingyi Kang, Yu Li, Sa Xie, Zehuan Yuan, and Jiashi Feng. Exploring balanced feature spaces for representation learning. In *International Conference on Learning Representations*, 2021. 1, 2
- [26] Bingyi Kang, Saining Xie, Marcus Rohrbach, Zhicheng Yan, Albert Gordo, Jiashi Feng, and Yannis Kalantidis. Decoupling representation and classifier for long-tailed recognition. In *International Conference on Learning Representations*, 2020. 1, 2, 3, 6, 7, 12
- [27] Yu Li, Tao Wang, Bingyi Kang, Sheng Tang, Chunfeng Wang, Jintao Li, and Jiashi Feng. Overcoming classifier imbalance for long-tail object detection with balanced group softmax. In *Computer Vision and Pattern Recognition*, 2020. 1
- [28] Ziwei Liu, Zhongqi Miao, Xiaohang Zhan, Jiayun Wang, Boqing Gong, and Stella X Yu. Large-scale long-tailed recognition in an open world. In *Computer Vision and Pattern Recognition*, pages 2537–2546, 2019. 6, 7, 12
- [29] Mingsheng Long, Jianmin Wang, Guiguang Ding, Jianguang Sun, and Philip S Yu. Transfer joint matching for unsupervised domain adaptation. In *Computer Vision and Pattern Recognition*, pages 1410–1417, 2014. 2
- [30] Aditya Krishna Menon, Sadeep Jayasumana, Ankit Singh Rawat, Himanshu Jain, Andreas Veit, and Sanjiv Kumar. Long-tail learning via logit adjustment. In *International Conference on Learning Representations*, 2021. 1, 2, 4
- [31] Prashant Pandey, Mrigank Raman, Sumanth Varambally, and Prathosh AP. Generalization on unseen domains via inference-time label-preserving target projections. In *Computer Vision and Pattern Recognition*, pages 12924–12933, 2021. 2

- [32] Seulki Park, Jongin Lim, Younghan Jeon, and Jin Young Choi. Influence-balanced loss for imbalanced visual classification. In *International Conference on Computer Vision*, 2021. 1
- [33] Yu Sun, Xiaolong Wang, Zhuang Liu, John Miller, Alexei Efros, and Moritz Hardt. Test-time training with self-supervision for generalization under distribution shifts. In *International Conference on Machine Learning*, 2020. 2
- [34] Jingru Tan, Changbao Wang, Buyu Li, Quanquan Li, Wanli Ouyang, Changqing Yin, and Junjie Yan. Equalization loss for long-tailed object recognition. In *Computer Vision and Pattern Recognition*, pages 11662–11671, 2020. 1
- [35] Kaihua Tang, Jianqiang Huang, and Hanwang Zhang. Long-tailed classification by keeping the good and removing the bad momentum causal effect. In *Advances in Neural Information Processing Systems*, volume 33, 2020. 6, 7, 16
- [36] Junjiao Tian, Yen-Cheng Liu, et al. Posterior re-calibration for imbalanced datasets. In *Advances in Neural Information Processing Systems*, 2020. 2
- [37] Grant Van Horn, Oisinand Mac Aodha, et al. The inaturalist species classification and detection dataset. In *Computer Vision and Pattern Recognition*, 2018. 6
- [38] Thomas Varsavsky, Mauricio Orbes-Arteaga, et al. Test-time unsupervised domain adaptation. In *International Conference on Medical Image Computing and Computer-Assisted Intervention*, pages 428–436, 2020. 2
- [39] Jiaqi Wang, Wenwei Zhang, Yuhang Zang, Yuhang Cao, Jiangmiao Pang, Tao Gong, Kai Chen, Ziwei Liu, Chen Change Loy, and Dahua Lin. Seesaw loss for long-tailed instance segmentation. In *Computer Vision and Pattern Recognition*, pages 9695–9704, 2021. 1
- [40] Peng Wang, Kai Han, et al. Contrastive learning based hybrid networks for long-tailed image classification. In *Computer Vision and Pattern Recognition*, 2021. 2
- [41] Xudong Wang, Long Lian, Zhongqi Miao, Ziwei Liu, and Stella X Yu. Long-tailed recognition by routing diverse distribution-aware experts. In *International Conference on Learning Representations*, 2021. 2, 3, 6, 7, 12, 13, 16, 17, 24
- [42] Yeming Wen, Dustin Tran, and Jimmy Ba. Batchensemble: an alternative approach to efficient ensemble and lifelong learning. In *International Conference on Learning Representations*, 2020. 24
- [43] Yandong Wen, Kaipeng Zhang, et al. A discriminative feature learning approach for deep face recognition. In *European Conference on Computer Vision*, 2016. 11
- [44] Zhenzhen Weng, Mehmet Giray Ogut, Shai Limonchik, and Serena Yeung. Unsupervised discovery of the long-tail in instance segmentation using hierarchical self-supervision. In *Computer Vision and Pattern Recognition*, 2021. 2
- [45] Liuyu Xiang, Guiguang Ding, and Jungong Han. Learning from multiple experts: Self-paced knowledge distillation for long-tailed classification. In *European Conference on Computer Vision*, 2020. 1, 2
- [46] Jason Yosinski, Jeff Clune, Yoshua Bengio, and Hod Lipson. How transferable are features in deep neural networks? In *Advances in Neural Information Processing Systems*, volume 27, pages 3320–3328, 2014. 4
- [47] Yuhang Zang, Chen Huang, and Chen Change Loy. Fasa: Feature augmentation and sampling adaptation for long-tailed instance segmentation. In *International Conference on Computer Vision*, 2021. 1
- [48] Songyang Zhang, Zeming Li, Shipeng Yan, Xuming He, and Jian Sun. Distribution alignment: A unified framework for long-tail visual recognition. In *Computer Vision and Pattern Recognition*, pages 2361–2370, 2021. 1
- [49] Yifan Zhang, Hanbo Chen, Ying Wei, Peilin Zhao, Jiezhong Cao, Xinjuan Fan, Xiaoying Lou, Hailing Liu, Jinlong Hou, Xiao Han, et al. From whole slide imaging to microscopy: Deep microscopy adaptation network for histopathology cancer image classification. In *International Conference on Medical Image Computing and Computer-Assisted Intervention*, pages 360–368, 2019. 2
- [50] Yifan Zhang, Bryan Hooi, Lanqing Hong, and Jiashi Feng. Unleashing the power of contrastive self-supervised visual models via contrast-regularized fine-tuning. In *Advances in Neural Information Processing Systems*, 2021. 2, 11
- [51] Yifan Zhang, Bingyi Kang, Bryan Hooi, Shuicheng Yan, and Jiashi Feng. Deep long-tailed learning: A survey. *ArXiv*, 2021. 1
- [52] Yifan Zhang, Ying Wei, et al. Collaborative unsupervised domain adaptation for medical image diagnosis. *IEEE Transactions on Image Processing*, 2020. 2
- [53] Yifan Zhang, Peilin Zhao, Jiezhong Cao, Wenye Ma, Junzhou Huang, Qingyao Wu, and Minghui Tan. Online adaptive asymmetric active learning for budgeted imbalanced data. In *ACM SIGKDD International Conference on Knowledge Discovery & Data Mining*, pages 2768–2777, 2018. 2
- [54] Peilin Zhao, Yifan Zhang, Min Wu, Steven CH Hoi, Minghui Tan, and Junzhou Huang. Adaptive cost-sensitive online classification. *IEEE Transactions on Knowledge and Data Engineering*, 31(2):214–228, 2018. 2
- [55] Zhisheng Zhong, Jiequan Cui, Shu Liu, and Jiaya Jia. Improving calibration for long-tailed recognition. In *Computer Vision and Pattern Recognition*, 2021. 3, 6, 7, 16, 17
- [56] Boyan Zhou, Quan Cui, Xiu-Shen Wei, and Zhao-Min Chen. Bbn: Bilateral-branch network with cumulative learning for long-tailed visual recognition. In *Computer Vision and Pattern Recognition*, pages 9719–9728, 2020. 1, 2, 6, 7, 12

Appendix

We organize the appendix as follows:

- Appendix **A**: the proofs for Theorem 1.
- Appendix **B**: the pseudo-code of the proposed method.
- Appendices **C-G**: Empirical settings and more results.

A. Proofs for Theorem 1

Proof. We first recall several key notations and define some new notations. The random variables of predictions and labels are defined as $\hat{Y} \sim p(\hat{y})$ and $Y \sim p(y)$, respectively. The number of classes is denoted by C . We further denote the test sample set of the class k by \mathcal{Z}_k , in which the total number of samples in this class is denoted by $|\mathcal{Z}_k|$. Let $c_k = \frac{1}{|\mathcal{Z}_k|} \sum_{\hat{y} \in \mathcal{Z}_k} \hat{y}$ represent the hard mean of all predictions of samples from the class k , and let $\stackrel{c}{=}$ indicate equality up to a multiplicative and/or additive constant.

As shown in Eq.(6), the optimization objective of our test-time self-supervised aggregation method is to maximize $\mathcal{S} = \sum_{j=1}^{n_t} \hat{y}_j^1 \cdot \hat{y}_j^2$, where n_t denotes the number of test samples. For convenience, we simplify the first data view to be the original data, so the objective function becomes $\sum_{j=1}^{n_t} \hat{y}_j \cdot \hat{y}_j^1$. Maximizing such an objective is equivalent to minimizing $\sum_{j=1}^{n_t} -\hat{y}_j \cdot \hat{y}_j^1$. Here, we assume the data augmentations are strong enough to generate representative data views that can simulate the test data from the same class. In this sense, the new data view can be regarded as an independent sample from the same class. Following this, we analyze our method by connecting $-\hat{y}_j \cdot \hat{y}_j^1$ to $\sum_{\hat{y}_j \in \mathcal{Z}_k} \|\hat{y}_j - c_k\|^2$, which is similar to the tightness term in the center loss [43]:

$$\begin{aligned}
& \sum_{\hat{y}_j, \hat{y}_j^1 \in \mathcal{Z}_k} -\hat{y}_j \cdot \hat{y}_j^1 \\
& \stackrel{c}{=} \frac{1}{|\mathcal{Z}_k|} \sum_{\hat{y}_j, \hat{y}_j^1 \in \mathcal{Z}_k} -\hat{y}_j \cdot \hat{y}_j^1 \\
& \stackrel{c}{=} \frac{1}{|\mathcal{Z}_k|} \sum_{\hat{y}_j, \hat{y}_j^1 \in \mathcal{Z}_k} \|\hat{y}_j\|^2 - \hat{y}_j \cdot \hat{y}_j^1 \\
& = \sum_{\hat{y}_j \in \mathcal{Z}_k} \|\hat{y}_j\|^2 - \frac{1}{|\mathcal{Z}_k|} \sum_{\hat{y}_j \in \mathcal{Z}_k} \sum_{\hat{y}_j^1 \in \mathcal{Z}_k} \hat{y}_j \cdot \hat{y}_j^1 \\
& = \sum_{\hat{y}_j \in \mathcal{Z}_k} \|\hat{y}_j\|^2 - 2 \frac{1}{|\mathcal{Z}_k|} \sum_{\hat{y}_j \in \mathcal{Z}_k} \sum_{\hat{y}_j^1 \in \mathcal{Z}_k} \hat{y}_j \cdot \hat{y}_j^1 \\
& \quad + \frac{1}{|\mathcal{Z}_k|} \sum_{\hat{y}_j \in \mathcal{Z}_k} \sum_{\hat{y}_j^1 \in \mathcal{Z}_k} \hat{y}_j \cdot \hat{y}_j^1 \\
& = \sum_{\hat{y}_j \in \mathcal{Z}_k} \|\hat{y}_j\|^2 - 2\hat{y}_j \cdot c_k + \|c_k\|^2 \\
& = \sum_{\hat{y}_j \in \mathcal{Z}_k} \|\hat{y}_j - c_k\|^2,
\end{aligned}$$

where we use the property of normalized predictions that $\|\hat{y}_j\|^2 = \|\hat{y}_j^2\|^2 = 1$ and the definition of the class hard mean $c_k = \frac{1}{|\mathcal{Z}_k|} \sum_{\hat{y} \in \mathcal{Z}_k} \hat{y}$.

By summing over all classes k , we obtain:

$$\sum_{j=1}^{n_t} -\hat{y}_j \cdot \hat{y}_j^1 \stackrel{c}{=} \sum_{j=1}^{n_t} \|\hat{y}_j - c_{y_i}\|^2.$$

Based on this equation, following [1, 50], we can interpret $\sum_{j=1}^{n_t} -\hat{y}_j \cdot \hat{y}_j^1$ as a conditional cross-entropy between \hat{Y} and another random variable \bar{Y} , whose conditional distribution given Y is a standard Gaussian centered around $c_Y: \bar{Y}|Y \sim \mathcal{N}(c_Y, i)$:

$$\sum_{j=1}^{n_t} -\hat{y}_j \cdot \hat{y}_j^1 \stackrel{c}{=} \mathcal{H}(\hat{Y}; \bar{Y}|Y) = \mathcal{H}(\hat{Y}|Y) + \mathcal{D}_{KL}(\hat{Y}||\bar{Y}|Y).$$

Hence, we know that $\sum_{j=1}^{n_t} -\hat{y}_j \cdot \hat{y}_j^1$ is an upper bound on the conditional entropy of predictions \hat{Y} given labels Y :

$$\sum_{j=1}^{n_t} -\hat{y}_j \cdot \hat{y}_j^1 \stackrel{c}{\geq} \mathcal{H}(\hat{Y}|Y),$$

where the symbol $\stackrel{c}{\geq}$ represents “larger than” up to a multiplicative and/or an additive constant. Moreover, when $\hat{Y}|Y \sim \mathcal{N}(c_Y, i)$, the bound is tight. As a result, minimizing $\sum_{j=1}^{n_t} -\hat{y}_j \cdot \hat{y}_j^1$ is equivalent to minimizing $\mathcal{H}(\hat{Y}|Y)$:

$$\sum_{j=1}^{n_t} -\hat{y}_j \cdot \hat{y}_j^1 \propto \mathcal{H}(\hat{Y}|Y). \quad (7)$$

Meanwhile, the mutual information between predictions \hat{Y} and labels Y can be represented by:

$$\mathcal{I}(\hat{Y}; Y) = \mathcal{H}(\hat{Y}) - \mathcal{H}(\hat{Y}|Y). \quad (8)$$

Combining Eqs.(7-8), we have:

$$\sum_{j=1}^{n_t} -\hat{y}_j \cdot \hat{y}_j^1 \propto -\mathcal{I}(\hat{Y}; Y) + \mathcal{H}(\hat{Y}).$$

Since $\mathcal{S} = \sum_{j=1}^{n_t} \hat{y}_j \cdot \hat{y}_j^1$, we obtain:

$$\mathcal{S} \propto \mathcal{I}(\hat{Y}; Y) - \mathcal{H}(\hat{Y}),$$

which concludes the proof for Theorem 1. \square

B. Pseudo-Code

This appendix provides pseudo-code of TADE, which consists of skill-diverse expert learning (c.f. Algorithm 1) and test-time self-supervised aggregation (c.f. Algorithm 2). For simplicity, we depict the pseudo-code based on batch size 1, while we conduct batch gradient descent in practice.

In Algorithm 2, to avoid the learned weight of some weak expert becoming zero, we give a stopping condition: if the weight for one expert is less than 0.05, we stop test-time training. Retaining a small amount of weight for each expert is sufficient to ensure the effect of ensemble learning.

Algorithm 1 Skill-diverse Expert Learning

Require: Epochs T ; Hyper-parameters λ for \mathcal{L}_{inv}
Initialize: Network backbone f_θ ; Experts E_1, E_2, E_3

```

1: for  $e=1, \dots, T$  do
2:   for  $x \in \mathcal{D}_s$  do // batch sampling in practice
3:     Obtain logits  $v_1$  based on  $f_\theta$  and  $E_1$ ;
4:     Obtain logits  $v_2$  based on  $f_\theta$  and  $E_2$ ;
5:     Obtain logits  $v_3$  based on  $f_\theta$  and  $E_3$ ;
6:     Compute loss  $\mathcal{L}_{ce}$  with  $v_1$  for Expert  $E_1$ ; // Eq.(1)
7:     Compute loss  $\mathcal{L}_{bal}$  with  $v_2$  for Expert  $E_2$ ; // Eq.(3)
8:     Compute loss  $\mathcal{L}_{inv}$  with  $v_3$  for Expert  $E_3$ ; // Eq.(5)
9:     Train the model with  $\mathcal{L}_{ce} + \mathcal{L}_{bal} + \mathcal{L}_{inv}$ .
10:  end for
11: end for
Output: The trained model  $\{f_\theta, E_1, E_2, E_3\}$ 

```

Algorithm 2 Test-time Self-supervised Aggregation

Require: Epochs T' ; The trained backbone f_θ ; The trained experts E_1, E_2, E_3
Initialize: Expert aggregation weights w // uniform initialization

```

1: for  $e=1, \dots, T'$  do
2:   for  $x \in \mathcal{D}_t$  do // batch sampling in practice
3:     Draw two data augmentation functions  $t \sim \mathcal{T}, t' \sim \mathcal{T}$ ;
4:     Generate data views  $x^1=t(x), x^2=t'(x)$ ;
5:     Obtain logits  $v_1^1, v_2^1, v_3^1$  for the view  $x^1$ ;
6:     Obtain logits  $v_1^2, v_2^2, v_3^2$  for the view  $x^2$ ;
7:     Normalize expert weights  $w$  via softmax function;
8:     Conduct predictions  $\hat{y}^1, \hat{y}^2$  based on  $\hat{y}=wv$ ;
9:     Compute prediction stability  $\mathcal{S}$ ; // Eq. (6)
10:    Maximize  $\mathcal{S}$  to update  $w$ ;
11:  end for
12:  If  $w_i \leq 0.05$  for any  $w_i \in w$ , then stop training.
13: end for
Output: Expert aggregation weights  $w$ 

```

C. More Experimental Settings

In this appendix, we provide more implementation details.

C.1. Test-agnostic Dataset Construction

Following [20], we construct three kinds of test class distributions, *i.e.*, the uniform distribution, forward long-tailed distributions and backward long-tailed distributions. In the backward ones, the long-tailed class order is flipped. Here, the forward and backward long-tailed test distributions contain multiple different imbalance ratios, *i.e.*, $\rho \in \{2, 5, 10, 25, 50\}$. Although the work [20] only constructs test data for ImageNet-LT, we use the same way to construct distribution-agnostic test datasets for other benchmark datasets, *i.e.*, CIFAR100-LT, Places-LT, iNaturalist 2018.

Considering the long-tailed training classes are sorted in a decreasing order, the various test datasets are constructed as follows: (1) Forward long-tailed distribution: the number of the j -th class is $n_j = N \cdot \rho^{(j-1)/C}$, where N is the sample number per class in the original test dataset and C is the number of classes. (2) Backward long-tailed distribution: the number of the j -th class is $n_j = N \cdot \rho^{(C-j)/C}$. In the backward distributions, the order of the long tail on classes is flipped, so the distribution shift between training and test data is large, especially with the rise of the imbalance ratio.

For ImageNet-LT, CIFAR100-LT and Places-LT, because of enough test samples per class, we follow the setting in [20] and construct the imbalance ratio set by $\rho \in \{2, 5, 10, 25, 50\}$. For iNaturalist 2018, each class only contains three test samples, so we adjust the imbalance ratio set to $\rho \in \{2, 3\}$. Note that, when we set $\rho = 3$, there are some classes in iNaturalist 2018 containing no test sample. *All these constructed distribution-agnostic datasets are publicly available along with our code.*

C.2. More Implementation Details of Our Method

We implement our method in PyTorch. Following [20, 41], we use ResNeXt-50 for ImageNet-LT, ResNet-32 for CIFAR100-LT, ResNet-152 for Places-LT and ResNet-50 for iNaturalist 2018 as backbones, while we use the cosine classifier for all datasets. In our method, the number of convolutional filters in each expert is reduced by 1/4, since by sharing the backbone and using fewer filters in each expert [41, 56], the computational complexity of the model is reduced compared to the model with independent experts.

In the training phase, the data augmentations are the same as existing methods [20, 26]. If not specified, for most datasets, we use the SGD optimizer with the momentum 0.9 and an initial learning rate of 0.1 (linear decay). More specifically, for ImageNet-LT, we train models for 180 epochs with batch size 64 and learning rate 0.025 (cosine decay). For CIFAR100-LT, the training epoch is 200 and the batch size is 128. For Places-LT, following [28], we use ResNet-152 pre-trained on ImageNet [11] as the backbone, where the batch size is 128 and the training epoch is 30. Moreover, the learning rate is 0.01 for the classifier and is 0.001 for all other layers. For iNaturalist 2018, we set the training epoch to 200, the batch size to 512 and the learning rate to 0.2. In the inverse softmax loss, we set $\lambda=2$ for ImageNet-LT and CIFAR100-LT, and set $\lambda=1$ for another two datasets.

In the test-time training, we use the same augmentations as MoCo v2 [6] to generate different data views, *i.e.*, random resized crop, color jitter, gray scale, Gaussian blur and horizontal flip. If not specified, we train the aggregation weights for 5 epochs with the batch size 128 using the same optimizer and learning rate as the training phase.

More detailed statistics of network architectures and hyper-parameters can be found in Table 10.

Items	ImageNet-LT	CIFAR100LT	Places-LT	iNaturalist 2018
Network Architectures				
network backbone	ResNeXt-50	ResNet-32	ResNet-152	ResNet-50
classifier	cosine classifier			
Training Phase				
epochs	180	200	30	200
batch size	64	128	128	512
learning rate (lr)	0.025	0.1	0.01	0.2
lr schedule	cosine decay	linear decay		
λ in inverse softmax loss	2		1	
weight decay factor	5×10^{-4}	5×10^{-4}	4×10^{-4}	2×10^{-4}
momentum factor	0.9			
optimizer	SGD optimizer with nesterov			
Test-time Training				
epochs	5			
batch size	128			
learning rate (lr)	0.025	0.1	0.01	0.1

Table 10. Statistics of the used network architectures and hyper-parameters in our method.

RIDE [41]																
Model	ImageNet-LT				CIFAR100-LT				Places-LT				iNaturalist 2018			
	Many	Med.	Few	All	Many	Med.	Few	All	Many	Med.	Few	All	Many	Med.	Few	All
Expert E_1	64.3	49.0	31.9	52.6	63.5	44.8	20.3	44.0	41.3	40.8	33.2	40.1	66.6	67.1	66.5	66.8
Expert E_2	64.7	49.4	31.2	52.8	63.1	44.7	20.2	43.8	43.0	40.9	33.6	40.3	66.1	67.1	66.6	66.8
Expert E_3	64.3	48.9	31.8	52.5	63.9	45.1	20.5	44.3	42.8	41.0	33.5	40.2	65.3	67.3	66.5	66.7
Ensemble	68.0	52.9	35.1	56.3	67.4	49.5	23.7	48.0	43.2	41.1	33.5	40.3	71.5	72.0	71.6	71.8

TADE (ours)																
Model	ImageNet-LT				CIFAR100-LT				Places-LT				iNaturalist 2018			
	Many	Med.	Few	All	Many	Med.	Few	All	Many	Med.	Few	All	Many	Med.	Few	All
Expert E_1	68.8	43.7	17.2	49.8	67.6	36.3	6.8	38.4	47.6	27.1	10.3	31.2	76.0	67.1	59.3	66.0
Expert E_2	65.5	50.5	33.3	53.9	61.2	44.7	23.5	44.2	42.6	42.3	32.3	40.5	69.2	70.7	69.8	70.2
Expert E_3	43.4	48.6	53.9	47.3	14.0	27.6	41.2	25.8	22.6	37.2	45.6	33.6	55.6	61.5	72.1	65.1
Ensemble	67.0	56.7	42.6	58.8	61.6	50.5	33.9	49.4	40.4	43.2	36.8	40.9	74.4	72.5	73.1	72.9

Table 11. Performance of each expert on the uniform test distribution. Here, the training imbalance ratio of CIFAR100-LT is 100. The results show that our proposed method can learn more skill-diverse experts, which lead to better performance of ensemble aggregation.

D. More Empirical Results

D.1. More Results on Skill-diverse Expert Learning

This appendix further evaluates the skill-diverse expert learning strategy on CIFAR100-LT, Places-LT and iNaturalist 2018 datasets. We report the results in Table 11, from which we draw the following observations. RIDE [41] is one of the state-of-the-art ensemble learning based methods and tries to learn diverse distribution-aware experts by maximizing the divergence among expert predictions. However, such a method cannot learn sufficiently diverse experts. As shown in Table 11, the three experts in RIDE perform very similarly on various groups of classes and have similar overall performance on all benchmark datasets. Such results show that simply maximizing the KL divergence of different experts' predictions is not sufficient to learn visibly diverse distribution-aware experts.

In contrast, our proposed method learns the skill-diverse experts by directly training each expert with their own corresponding expertise-guided loss. To be specific, the forward expert seeks to learn the long-tailed training distribution, so we directly train it with the cross-entropy loss. For the uniform expert, we use the balanced softmax loss to simulate the uniform test distribution. For the backward expert, we design a novel inverse softmax loss to train the expert so that it can simulate the inversely long-tailed class distribution. Table 11 shows that the three experts trained by our method are visibly diverse and skilled in handling different class distributions. Specifically, the forward expert is skilled in many-shot classes, the uniform expert is more balanced with higher overall performance, and the backward expert is good at few-shot classes. Because of such a novel design that enhances expert diversity, our method is able to obtain more promising performance compared to RIDE.

Test Dist.	ImageNet-LT			CIFAR100-LT(IR10)			CIFAR100-LT(IR50)		
	E1 (w_1)	E2 (w_2)	E3 (w_3)	E1 (w_1)	E2 (w_2)	E3 (w_3)	E1 (w_1)	E2 (w_2)	E3 (w_3)
Forward-LT-50	0.52	0.35	0.13	0.53	0.38	0.09	0.55	0.38	0.07
Forward-LT-25	0.50	0.35	0.15	0.52	0.37	0.11	0.54	0.38	0.08
Forward-LT-10	0.46	0.36	0.18	0.47	0.36	0.17	0.52	0.37	0.11
Forward-LT-5	0.43	0.34	0.23	0.46	0.34	0.20	0.50	0.36	0.14
Forward-LT-2	0.37	0.35	0.28	0.39	0.37	0.24	0.39	0.38	0.23
Uniform	0.33	0.33	0.34	0.38	0.32	0.3	0.35	0.33	0.33
Backward-LT-2	0.29	0.31	0.40	0.35	0.33	0.31	0.30	0.30	0.40
Backward-LT-5	0.24	0.31	0.45	0.31	0.32	0.37	0.21	0.29	0.50
Backward-LT-10	0.21	0.29	0.50	0.26	0.32	0.42	0.20	0.29	0.51
Backward-LT-25	0.18	0.29	0.53	0.24	0.30	0.46	0.18	0.27	0.55
Backward-LT-50	0.17	0.27	0.56	0.23	0.28	0.49	0.14	0.24	0.62

Test Dist.	CIFAR100-LT(IR100)			Places-LT			iNaturalist 2018		
	E1 (w_1)	E2 (w_2)	E3 (w_3)	E1 (w_1)	E2 (w_2)	E3 (w_3)	E1 (w_1)	E2 (w_2)	E3 (w_3)
Forward-LT-50	0.56	0.38	0.06	0.50	0.20	0.20	-	-	-
Forward-LT-25	0.55	0.38	0.07	0.50	0.20	0.20	-	-	-
Forward-LT-10	0.52	0.39	0.09	0.50	0.20	0.20	-	-	-
Forward-LT-5	0.51	0.37	0.12	0.46	0.32	0.22	-	-	-
Forward-LT-2	0.49	0.35	0.16	0.40	0.34	0.26	0.41	0.34	0.25
Uniform	0.40	0.35	0.24	0.25	0.34	0.41	0.33	0.33	0.34
Backward-LT-2	0.33	0.31	0.36	0.18	0.30	0.52	0.28	0.32	0.40
Backward-LT-5	0.28	0.30	0.42	0.17	0.28	0.55	-	-	-
Backward-LT-10	0.23	0.28	0.49	0.17	0.27	0.56	-	-	-
Backward-LT-25	0.21	0.26	0.53	0.17	0.27	0.56	-	-	-
Backward-LT-50	0.16	0.28	0.56	0.17	0.27	0.56	-	-	-

Table 12. The learned aggregation weights by our test-time self-supervised aggregation strategy under different test class distributions on ImageNet-LT, CIFAR100-LT, Places-LT and iNaturalist 2018. The results show that our method can learn suitable expert weights for various test class distributions.

D.2. More Results on Test-time Expert Aggregation

This appendix provides more results to examine the effectiveness of test-time expert aggregation. We report results in Tables 12, from which we draw several observations.

First of all, our method is able to learn suitable expert aggregation weights for arbitrary test class distributions, without knowing any test distribution prior. For the forward long-tailed test distribution, where the test data number of many-shot classes is more than that of medium-shot and few-shot classes, our method learns a higher weight for the forward expert E_1 who is skilled in many-shot classes, and learns relatively low weights for the expert E_2 and expert E_3 who are good at medium-shot and few-shot classes. Meanwhile, for the uniform test class distribution where all classes have the same number of test samples, our test-time expert aggregation strategy learns relatively balanced weights for the three experts. For example, on the uniform ImageNet-LT test data, the learned weights by our strategy are 0.33, 0.33 and 0.34 for the three experts, respectively. In addition, for the backward long-tailed test distributions, our method learns a higher weight for the backward expert E_3 and a relatively low weight for the forward expert E_1 . Note that when the class imbalance ratio becomes larger, our method is able to learn more diverse expert weights adaptively for fitting the actual test class distributions.

Such results not only demonstrate the effectiveness of our strategy, but also verify the theoretical analysis that our method can simulate the unknown test class distribution. To our knowledge, such an ability is quite promising, since it is difficult to know the practical test class distributions in real-world tasks. This implies that our method is a better candidate to handle real-world long-tailed applications.

Relying on the learned expert weights, our method aggregates the three experts appropriately and thus obtains promising performance gains on various test distributions, as shown in Table 13. Note that the performance gain compared to existing methods gets larger as the test dataset gets more imbalanced. For example, on CIFAR100-LT with the imbalance ratio of 50, our test-time self-supervised aggregation strategy obtains 7.7% performance gain on the Forward-LT-50 distribution and 9.2% performance gain on the Backward-LT-50 distribution, both of which are non-trivial.

In addition, since the imbalance degrees of the test datasets are relatively low on iNaturalist 2018, the simulated test class distributions are thus relatively balanced. As a result, the obtained performance improvement is not that significant, compared to other datasets. Even so, if there are more iNaturalist test samples following highly imbalanced test class distributions in practical applications, our method can obtain more promising results.

Test Dist.	ImageNet-LT								CIFAR100-LT(IR10)							
	Ours w/o test-time aggregation				Ours w/ test-time aggregation				Ours w/o test-time aggregation				Ours w/ test-time aggregation			
	Many	Med.	Few	All	Many	Med.	Few	All	Many	Med.	Few	All	Many	Med.	Few	All
Forward-LT-50	65.6	55.7	44.1	65.5	70.0	53.2	33.1	69.4 (+3.9)	66.3	58.3	-	66.3	69.0	50.8	-	71.2 (+4.9)
Forward-LT-25	65.3	56.9	43.5	64.4	69.5	53.2	32.2	67.4 (+3.0)	63.1	60.8	-	64.5	67.6	52.2	-	69.4 (+4.9)
Forward-LT-10	66.5	56.8	44.2	63.6	69.9	54.3	34.7	65.4 (+1.8)	64.1	58.8	-	64.1	67.2	54.2	-	67.6 (+3.5)
Forward-LT-5	65.9	56.5	43.3	62.0	68.9	54.8	35.8	63.0 (+1.0)	62.7	57.1	-	62.7	66.9	54/3	-	66.3 (+3.6)
Forward-LT-2	66.2	56.5	42.1	60.0	68.2	56.0	40.1	60.6 (+0.6)	62.8	56.3	-	61.6	66.1	56.6	-	64.4 (+2.8)
Uniform	67.0	56.7	42.6	58.8	66.5	57.0	43.5	58.8 (+0.0)	65.5	59.9	-	63.6	65.8	58.8	-	63.6 (+0.0)
Backward-LT-2	66.3	56.7	43.1	56.8	65.3	57.1	45.0	57.1 (+0.3)	62.7	56.9	-	60.2	65.6	59.5	-	62.9 (+2.7)
Backward-LT-5	66.6	56.9	43.0	54.7	63.4	56.4	47.5	55.5 (+0.8)	62.8	57.5	-	59.7	65.1	60.4	-	62.4 (+2.7)
Backward-LT-10	65.0	57.6	43.1	53.1	60.9	57.5	50.1	54.5 (+1.4)	63.5	58.2	-	59.8	62.5	61.4	-	61.7 (+1.9)
Backward-LT-25	64.2	56.9	43.4	51.1	60.5	57.1	50.0	53.7 (+2.6)	63.4	57.7	-	58.7	61.9	62.0	-	62.1 (+3.4)
Backward-LT-50	69.1	57.0	42.9	49.8	60.7	56.2	50.7	53.1 (+3.3)	62.0	57.8	-	58.6	62.6	62.6	-	63.0 (+3.8)

Test Dist.	CIFAR100-LT(IR50)								CIFAR100-LT(IR100)							
	Ours w/o test-time aggregation				Ours w/ test-time aggregation				Ours w/o test-time aggregation				Ours w/ test-time aggregation			
	Many	Med.	Few	All	Many	Med.	Few	All	Many	Med.	Few	All	Many	Med.	Few	All
Forward-LT-50	59.7	53.3	26.9	59.5	68.0	44.1	19.4	67.2 (+7.7)	60.7	50.3	32.4	58.4	69.9	48.8	14.2	65.9 (+7.5)
Forward-LT-25	59.1	51.8	32.6	58.6	67.3	46.2	19.5	64.5 (+6.9)	60.6	49.6	29.4	57.0	68.9	46.5	15.1	62.5 (+5.5)
Forward-LT-10	59.7	47.2	36.1	56.4	67.2	45.7	24.7	61.2 (+4.8)	60.1	48.6	28.4	54.4	68.3	46.9	16.7	58.3 (+3.9)
Forward-LT-5	59.7	46.9	36.9	54.8	67.0	45.7	29.9	58.6 (+3.4)	60.3	50.3	29.5	53.1	68.3	45.3	19.4	54.8 (+1.7)
Forward-LT-2	59.2	48.4	41.9	53.2	63.8	48.5	39.3	55.4 (+2.2)	60.6	48.8	31.3	50.1	68.2	47.6	22.5	51.1 (+1.0)
Uniform	61.0	50.2	45.7	53.8	61.5	50.2	45.0	53.9 (+0.1)	61.6	50.5	33.9	49.4	65.4	49.3	29.3	49.8 (+0.4)
Backward-LT-2	59.0	48.2	42.8	50.1	57.5	49.7	49.4	51.9 (+1.8)	61.2	49.1	30.8	45.2	63.1	49.4	31.7	46.2 (+1.0)
Backward-LT-5	60.1	48.6	41.8	48.2	50.0	49.3	54.2	50.9 (+2.7)	62.0	48.9	32.0	42.6	56.2	49.1	38.2	44.7 (+2.1)
Backward-LT-10	58.6	46.9	42.6	46.1	49.3	49.1	54.6	51.0 (+4.9)	60.6	48.2	31.7	39.7	52.1	47.9	40.6	43.9 (+4.2)
Backward-LT-25	55.1	48.9	41.2	44.4	44.5	46.6	57.0	51.7 (+7.3)	58.2	47.9	32.2	36.7	48.7	44.2	41.8	42.5 (+5.8)
Backward-LT-50	57.0	48.8	41.6	43.6	45.8	46.6	58.4	52.8 (+9.2)	66.9	48.6	30.4	35.0	49.0	42.7	42.5	42.4 (+7.4)

Test Dist.	Places-LT								iNaturalist 2018							
	Ours w/o test-time aggregation				Ours w/ test-time aggregation				Ours w/o test-time aggregation				Ours w/ test-time aggregation			
	Many	Med.	Few	All	Many	Med.	Few	All	Many	Med.	Few	All	Many	Med.	Few	All
Forward-LT-50	43.5	42.5	65.9	43.7	46.8	39.3	30.5	46.4 (+2.7)	-	-	-	-	-	-	-	-
Forward-LT-25	42.8	42.1	29.3	42.7	46.3	38.9	23.6	44.9 (+2.3)	-	-	-	-	-	-	-	-
Forward-LT-10	42.3	41.9	34.9	42.3	45.4	39.0	27.0	43.3 (+1.0)	-	-	-	-	-	-	-	-
Forward-LT-5	43.0	44.0	33.1	42.4	45.6	40.6	27.3	42.6 (+0.2)	-	-	-	-	-	-	-	-
Forward-LT-2	43.4	42.4	32.6	41.3	44.9	41.2	29.5	41.3 (+0.0)	73.9	72.4	72.0	72.4	75.5	72.5	70.7	72.5 (+0.1)
Uniform	43.1	42.4	33.2	40.9	40.4	43.2	36.8	40.9 (+0.0)	74.4	72.5	73.1	72.9	74.5	72.5	73.0	72.9 (+0.0)
Backward-LT-2	42.8	41.9	33.2	39.9	37.1	42.9	40.0	40.6 (+0.7)	76.1	72.8	72.6	73.1	74.9	72.6	73.7	73.5 (+0.4)
Backward-LT-5	43.1	42.0	33.6	39.1	36.4	42.7	41.1	41.1 (+2.0)	-	-	-	-	-	-	-	-
Backward-LT-10	43.5	42.9	33.7	38.9	35.2	43.2	41.3	41.4 (+2.5)	-	-	-	-	-	-	-	-
Backward-LT-25	44.6	42.4	33.6	37.8	38.0	43.5	41.1	42.0 (+4.2)	-	-	-	-	-	-	-	-
Backward-LT-50	42.2	43.4	33.3	37.2	37.3	43.5	40.5	41.6 (+4.7)	-	-	-	-	-	-	-	-

Table 13. The performance improvement via test-time self-supervised aggregation under various test class distributions on ImageNet-LT, CIFAR100-LT, Places-LT and iNaturalist 2018.

Method	ImageNet-LT				CIFAR100-LT(IR10)				CIFAR100-LT(IR50)			
	Many	Med.	Few	All	Many	Med.	Few	All	Many	Med.	Few	All
Softmax	68.1	41.5	14.0	48.0	66.0	42.7	-	59.1	66.8	37.4	15.5	45.6
Causal [35]	64.1	45.8	27.2	50.3	63.3	49.9	-	59.4	62.9	44.9	26.2	48.8
Balanced Softmax [23]	64.1	48.2	33.4	52.3	43.4	55.7	-	61.0	62.1	45.6	36.7	50.9
MiSLAS [55]	62.0	49.1	32.8	51.4	64.9	56.6	-	62.5	61.8	48.9	33.9	51.5
LADE [20]	64.4	47.7	34.3	52.3	63.8	56.0	-	61.6	60.2	46.2	35.6	50.1
RIDE [41]	68.0	52.9	35.1	56.3	65.7	53.3	-	61.8	66.6	46.2	30.3	51.7
TADE (ours)	66.5	57.0	43.5	58.8	65.8	58.8	-	63.6	61.5	50.2	45.0	53.9

Method	CIFAR100-LT(IR100)				Places-LT				iNaturalist 2018			
	Many	Med.	Few	All	Many	Med.	Few	All	Many	Med.	Few	All
Softmax	68.6	41.1	9.6	41.4	46.2	27.5	12.7	31.4	74.7	66.3	60.0	64.7
Causal [35]	64.1	46.8	19.9	45.0	23.8	35.7	39.8	32.2	71.0	66.7	59.7	64.4
Balanced Softmax [23]	59.5	45.4	30.7	46.1	42.6	39.8	32.7	39.4	70.9	70.7	70.4	70.6
MiSLAS [55]	60.4	49.6	26.6	46.8	41.6	39.3	27.5	37.6	71.7	71.5	69.7	70.7
LADE [20]	58.7	45.8	29.8	45.6	42.6	39.4	32.3	39.2	68.9	68.7	70.2	69.3
RIDE [41]	67.4	49.5	23.7	48.0	43.1	41.0	33.0	40.3	71.5	70.0	71.6	71.8
TADE (ours)	65.4	49.3	29.3	49.8	40.4	43.2	36.8	40.9	74.5	72.5	73.0	72.9

Table 14. Top-1 accuracy of long-tailed recognition methods on the uniform test distribution.

Methods	ImageNet-LT	CIFAR100-LT(IR10)	CIFAR100-LT(IR50)	CIFAR100-LT(IR100)	Places-LT	iNaturalist 2018
PaCo* [9]	58.2	64.2	56.0	52.0	41.2	73.2
TADE* (ours)	61.2	65.3	57.3	52.2	41.3	74.5

Table 15. Accuracy of long-tailed methods with stronger augmentation, where the test class distribution is uniform. Here, * denotes training with RandAugment [8] for 400 epochs. The baseline results are directly copied from the work [9].

Dataset	Backbone	Many	Med.	Few	All
ImageNet-LT	ResNeXt-50	66.5	57.0	43.5	58.8
	ResNeXt-50*	67.3	60.4	46.4	61.2
	ResNeXt-101	66.8	57.5	43.1	59.1
	ResNeXt-101*	68.1	60.5	45.5	61.4
	ResNeXt-152	67.2	57.4	43.5	59.3
	ResNeXt-152*	68.6	61.2	47.0	62.1
iNaturalist 2018	ResNet-50	74.5	72.5	73.0	72.9
	ResNet-50*	75.5	73.7	75.1	74.5
	ResNet-152	76.2	64.3	65.1	74.8
	ResNet-152*	78.3	77.0	76.7	77.0

Table 16. Accuracy of TADE with various network architectures. Here, * denotes training with RandAugment [8] for 400 epochs.

D.3. More Results on Uniform Test Distribution

In the main paper, we provide the average performance over all classes on the uniform test class distribution. Here, we further report the accuracy regarding class subsets (c.f. Table 14), which makes the results more complete.

Moreover, inspired by [9], we further evaluate TADE when training with stronger data augmentation (*i.e.*, RandAugment [8]) for 400 epochs. The results in Table 15 further demonstrate the state-of-the-art performance of TADE.

In addition to using the widely-used network backbones, we further evaluate TADE with various backbones. The results in Table 16 not only show the promising performance of TADE, but also demonstrate that TADE is able to train different network backbones well.

Imbalance Ratio	Softmax	BBN	MiSLAS	RIDE	TADE (ours)
10	86.4	88.4	90.0	89.7	90.8
100	70.4	79.9	82.1	81.6	83.8

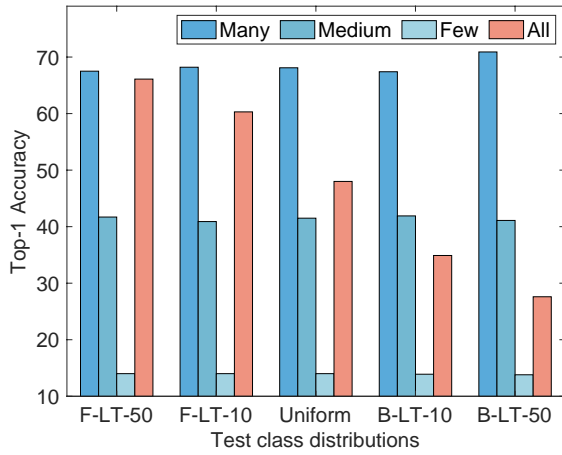
Table 17. Accuracy on CIFAR10-LT, where the test class distribution is uniform. Most results are directly copied from the work [55].

We also conduct experiments on CIFAR10-LT with imbalance ratios 10 and 100. Promising results in Table 17 further demonstrate the effectiveness of our proposed method.

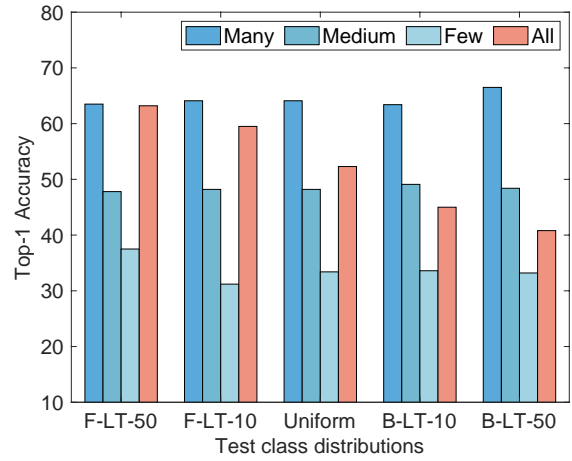
D.4. More Results on Test-agnostic Distributions

The main paper provides the overall performance on various test class distributions, while this appendix further reports the accuracy regarding three class subsets. As shown in Table 13, by using the test-time self-supervised aggregation strategy, our method achieves better performance on the dominant test classes, thus obtaining better performance on various test class distributions. Such an observation can also be supported by the visualization result of Figure 4, which plots the results of existing methods on ImageNet-LT with different test class distributions regarding three class subsets.

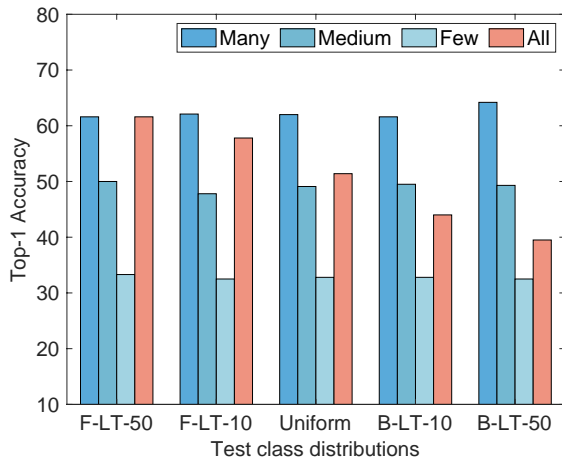
We also plot the results with different test class distributions in Figure 5. Softmax only performs well on highly-imbalanced forward long-tailed class distributions. Existing long-tailed baselines outperform Softmax, but they cannot handle backward test class distributions well. In contrast, our method consistently outperforms baselines on all benchmark datasets, particularly under the backward long-tailed test distributions with a relatively large imbalance ratio.



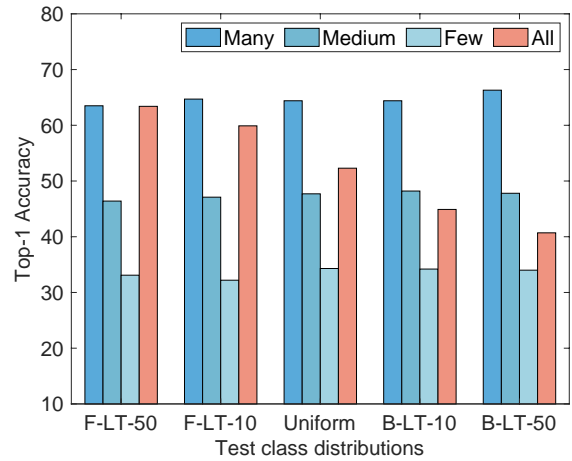
(a) Softmax



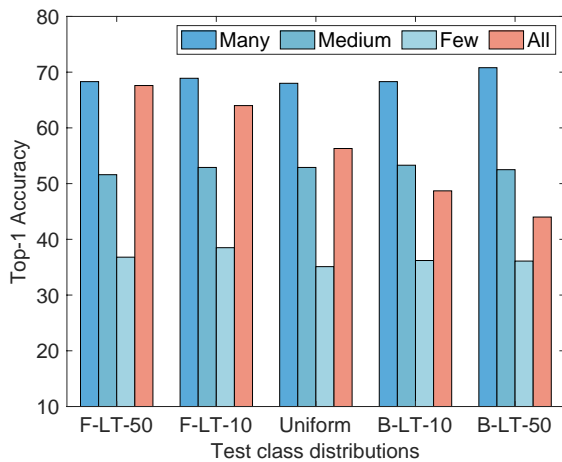
(b) Balanced Softmax [23]



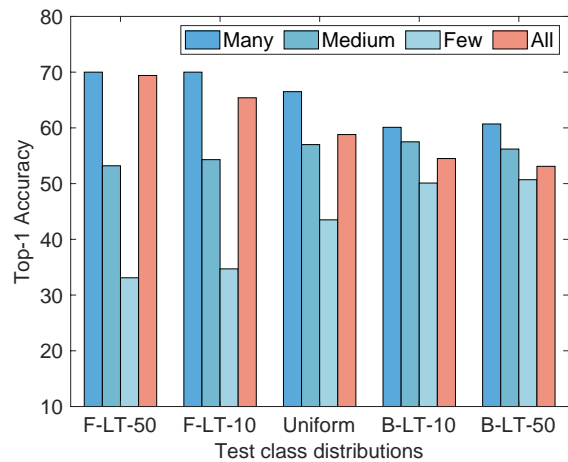
(c) MiSLAS [55]



(d) LADE w/o prior [20]

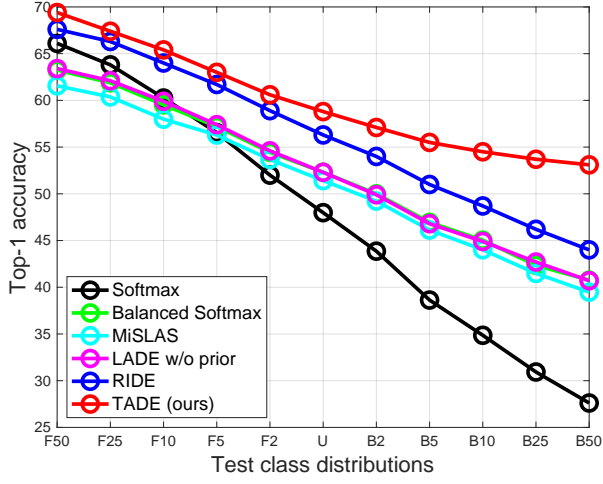


(e) RIDE [41]

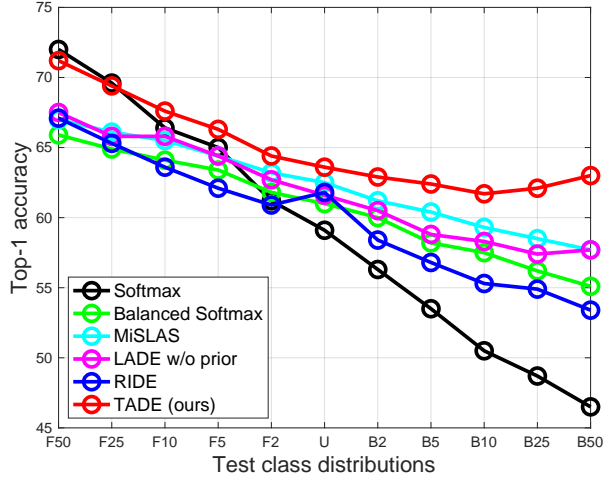


(f) TADE (ours)

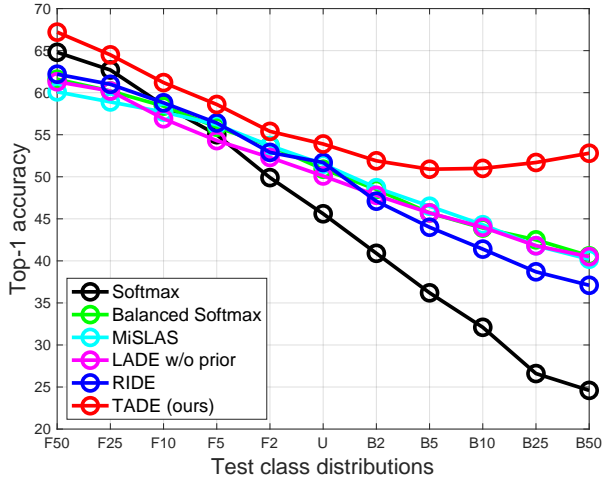
Figure 4. Top-1 accuracy on ImageNet-LT with different test class distributions, including uniform, forward and backward long-tailed ones with imbalance ratios 10 and 50, respectively. Here, “F-LT- N ” and “B-LT- N ” indicate the cases where test samples follow the same long-tailed distribution as training data and inversely long-tailed to the training data, with the imbalance ratio N , respectively. The results show that **existing methods perform very similarly on different test class distributions in terms of their performance on many-shot, medium-shot and few-shot classes. In contrast, our proposed method can adapt to arbitrary test class distributions in terms of many-shot, medium-shot and few-shot performance, thus leading to better overall performance on each test class distribution.**



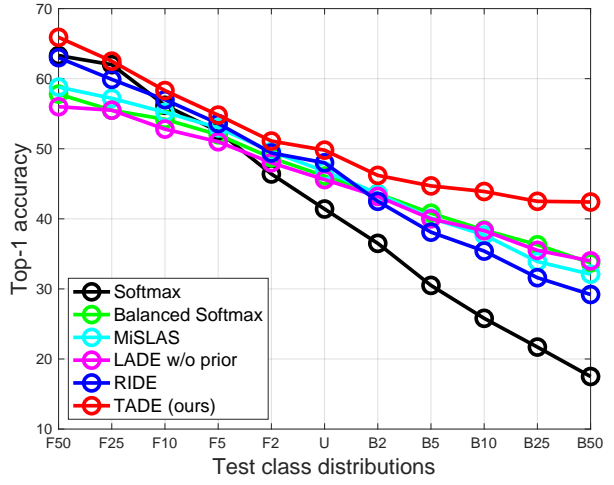
(a) ImageNet-LT



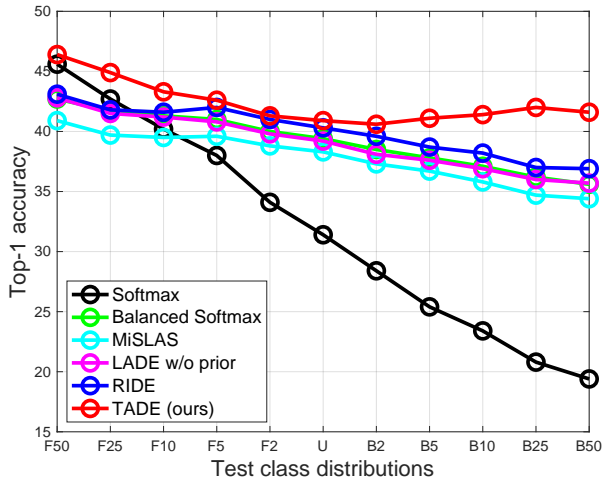
(b) CIFAR100-LT(IR10)



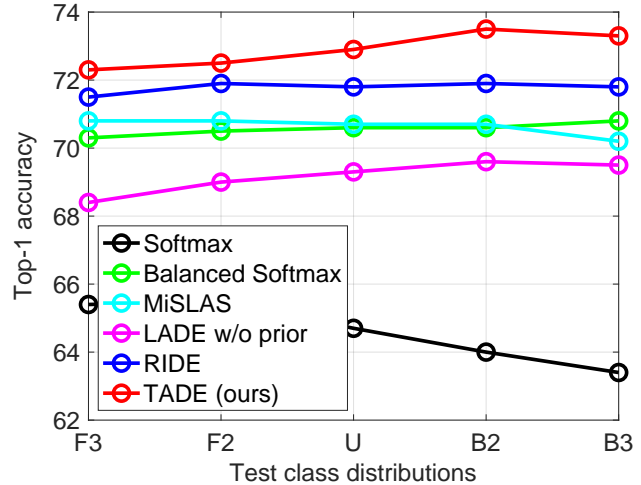
(c) CIFAR100-LT(IR50)



(d) CIFAR100-LT(IR100)



(e) Places-LT



(f) iNaturalist 2018

Figure 5. Performance visualizations on various unknown test class distributions, where “F” indicates the forward long-tailed distributions as training data, “B” indicates the backward long-tailed distributions to the training data, and “U” denotes the uniform distribution.

E. Ablation Studies on Expert Learning

E.1. Discussion on Expert Number

Our approach can be straightforwardly extended to more than three experts. For the models with more experts, we can adjust the hyper-parameters in the expertise-guided loss functions so that different experts are skilled in different types of class distributions. Following this observation, we further test the influence of the expert number on our method. As shown in Table 18, with the increasing number of experts, the ensemble performance of our method is improved, *e.g.*, four experts can obtain 1.2% performance gain compared to three experts.

In TADE, we consider three experts because the “forward” and “backward” experts are necessary since they span a wide spectrum of possible test class distributions, while the “uniform” expert ensures that we retain high accuracy on the uniform test class distributions. Note that three experts are sufficient to provide a good trade-off between performance and efficiency.

Model	3 experts			
	Many-shot	Medium-shot	Few-shot	All classes
Expert E_1	68.8	43.7	17.2	49.8
Expert E_2	65.5	50.5	33.3	53.9
Expert E_3	43.4	48.6	53.9	47.3
Ensemble	67.0	56.7	42.6	58.8

Model	4 experts			
	Many-shot	Medium-shot	Few-shot	All classes
Expert E_1	69.4	44.5	16.5	50.3
Expert E_2	66.2	51.5	32.9	54.6
Expert E_3	55.7	52.7	46.8	53.4
Expert E_4	44.1	49.7	55.9	48.4
Ensemble	66.6	58.4	46.7	60.0

Model	5 experts			
	Many-shot	Medium-shot	Few-shot	All classes
Expert E_1	69.8	44.9	17.0	50.7
Expert E_2	68.8	48.4	23.9	52.9
Expert E_3	66.1	51.4	22.0	54.5
Expert E_4	56.8	52.7	47.7	53.6
Expert E_5	43.1	59.0	54.8	47.5
Ensemble	68.8	58.5	43.2	60.4

Model	6 experts			
	Many-shot	Medium-shot	Few-shot	All classes
Expert E_1	69.0	35.1	6.51	44.3
Expert E_2	69.6	44.3	16.6	50.3
Expert E_3	66.0	51.2	32.2	54.3
Expert E_4	56.1	52.5	47.4	53.2
Expert E_5	43.2	49.2	55.5	47.8
Expert E_6	31.6	43.8	58.3	41.0
Ensemble	66.9	59.4	46.5	60.5

Table 18. Performance of our method with different numbers of experts on ImageNet-LT under the uniform test distribution.

E.2. Hyper-parameters in Inverse Softmax Loss

This appendix evaluates the influence of the hyper-parameter λ in the inverse softmax loss for the backward expert, where we fix other hyper-parameters and only adjust the value of λ . As shown in Table 19, with the increase of λ , the backward expert simulates more inversely long-tailed distribution (to the training data), and thus the ensemble performance on few-shot classes is better. Moreover, when $\lambda \in \{2, 3\}$, our method achieves a better trade-off between head classes and tail classes, leading to relatively better overall performance on ImageNet-LT.

Model	$\lambda = 0.5$			
	Many-shot	Medium-shot	Few-shot	All classes
Expert E_1	69.1	43.6	17.2	49.8
Expert E_2	66.4	50.9	33.4	54.5
Expert E_3	61.9	51.9	40.3	54.2
Ensemble	71.0	54.6	33.4	58.0

Model	$\lambda = 1$			
	Many-shot	Medium-shot	Few-shot	All classes
Expert E_1	69.7	44.0	16.8	50.2
Expert E_2	65.5	51.1	32.4	54.4
Expert E_3	56.5	52.3	47.1	53.2
Ensemble	77.2	55.7	36.2	58.6

Model	$\lambda = 2$			
	Many-shot	Medium-shot	Few-shot	All classes
Expert E_1	68.8	43.7	17.2	49.8
Expert E_2	65.5	50.5	33.3	53.9
Expert E_3	43.4	48.6	53.9	47.3
Ensemble	67.0	56.7	42.6	58.8

Model	$\lambda = 3$			
	Many-shot	Medium-shot	Few-shot	All classes
Expert E_1	69.6	43.8	17.4	50.2
Expert E_2	66.2	50.7	33.1	54.2
Expert E_3	43.4	48.6	53.9	48.0
Ensemble	67.8	56.8	42.4	59.1

Model	$\lambda = 4$			
	Many-shot	Medium-shot	Few-shot	All classes
Expert E_1	69.1	44.1	16.3	49.9
Expert E_2	65.7	50.8	32.6	54.1
Expert E_3	21.9	38.1	58.9	34.7
Ensemble	60.2	57.5	50.4	57.6

Model	$\lambda = 5$			
	Many-shot	Medium-shot	Few-shot	All classes
Expert E_1	69.7	43.7	16.5	50.0
Expert E_2	65.9	50.9	33.0	54.2
Expert E_3	16.0	33.9	60.6	30.6
Ensemble	56.3	57.5	54.0	56.6

Table 19. Influence of the hyper-parameter λ in the inverse softmax loss on ImageNet-LT under the uniform test distribution.

Test Dist.	Epoch 1			Epoch 5			Epoch 10		
	E1 (w_1)	E2 (w_2)	E3 (w_3)	E1 (w_1)	E2 (w_2)	E3 (w_3)	E1 (w_1)	E2 (w_2)	E3 (w_3)
Forward-LT-50	0.44	0.33	0.23	0.52	0.35	0.13	0.52	0.37	0.11
Forward-LT-25	0.43	0.34	0.23	0.50	0.35	0.15	0.50	0.37	0.13
Forward-LT-10	0.43	0.34	0.23	0.46	0.36	0.18	0.46	0.36	0.18
Forward-LT-5	0.41	0.34	0.25	0.43	0.34	0.23	0.43	0.35	0.22
Forward-LT-2	0.37	0.33	0.30	0.37	0.35	0.28	0.38	0.33	0.29
Uniform	0.34	0.31	0.35	0.33	0.33	0.34	0.33	0.32	0.35
Backward-LT-2	0.30	0.32	0.38	0.29	0.31	0.40	0.29	0.32	0.39
Backward-LT-5	0.27	0.29	0.44	0.24	0.31	0.45	0.23	0.31	0.46
Backward-LT-10	0.24	0.29	0.47	0.21	0.29	0.50	0.21	0.30	0.49
Backward-LT-25	0.23	0.29	0.48	0.18	0.29	0.53	0.17	0.3	0.53
Backward-LT-50	0.24	0.29	0.47	0.17	0.27	0.56	0.15	0.28	0.57

Test Dist.	Epoch 20			Epoch 50			Epoch 100		
	E1 (w_1)	E2 (w_2)	E3 (w_3)	E1 (w_1)	E2 (w_2)	E3 (w_3)	E1 (w_1)	E2 (w_2)	E3 (w_3)
Forward-LT-50	0.53	0.38	0.09	0.53	0.38	0.09	0.53	0.38	0.09
Forward-LT-25	0.51	0.37	0.12	0.52	0.37	0.11	0.50	0.38	0.12
Forward-LT-10	0.44	0.36	0.20	0.45	0.37	0.18	0.46	0.36	0.18
Forward-LT-5	0.42	0.35	0.23	0.42	0.35	0.23	0.42	0.35	0.23
Forward-LT-2	0.38	0.33	0.29	0.39	0.33	0.28	0.38	0.32	0.30
Uniform	0.33	0.33	0.34	0.34	0.32	0.34	0.32	0.33	0.35
Backward-LT-2	0.29	0.31	0.40	0.30	0.32	0.38	0.29	0.30	0.41
Backward-LT-5	0.24	0.31	0.45	0.23	0.29	0.48	0.25	0.30	0.45
Backward-LT-10	0.20	0.30	0.50	0.21	0.31	0.48	0.21	0.30	0.49
Backward-LT-25	0.16	0.30	0.54	0.17	0.29	0.54	0.17	0.30	0.53
Backward-LT-50	0.15	0.29	0.56	0.14	0.29	0.57	0.14	0.29	0.57

Table 20. The influence of the epoch number on the learned expert weights by test-time self-supervised aggregation on ImageNet-LT.

Test Dist.	Batch size 64			Batch size 128			Batch size 256		
	E1 (w_1)	E2 (w_2)	E3 (w_3)	E1 (w_1)	E2 (w_2)	E3 (w_3)	E1 (w_1)	E2 (w_2)	E3 (w_3)
Forward-LT-50	0.52	0.37	0.11	0.52	0.35	0.13	0.50	0.33	0.17
Forward-LT-25	0.49	0.38	0.13	0.50	0.35	0.15	0.48	0.24	0.18
Forward-LT-10	0.46	0.36	0.18	0.46	0.36	0.18	0.45	0.35	0.20
Forward-LT-5	0.44	0.34	0.22	0.43	0.34	0.23	0.43	0.35	0.22
Forward-LT-2	0.37	0.34	0.29	0.37	0.35	0.28	0.38	0.33	0.29
Uniform	0.34	0.32	0.34	0.33	0.33	0.34	0.33	0.32	0.35
Backward-LT-2	0.28	0.32	0.40	0.29	0.31	0.40	0.30	0.31	0.39
Backward-LT-5	0.24	0.30	0.46	0.24	0.31	0.45	0.25	0.30	0.45
Backward-LT-10	0.21	0.30	0.49	0.21	0.29	0.50	0.22	0.29	0.49
Backward-LT-25	0.17	0.29	0.54	0.18	0.29	0.53	0.20	0.28	0.52
Backward-LT-50	0.15	0.30	0.55	0.17	0.27	0.56	0.19	0.27	0.54

Table 21. The influence of the batch size on the learned expert weights by test-time self-supervised aggregation on ImageNet-LT.

F. Ablation Studies on Test-time Aggregation

F.1. Influences of Training Epoch

In previous results, we set the training epoch of test-time self-supervised aggregation to 5 on all datasets. Here, we further evaluate the influence of the epoch number, where we adjust the epoch number from 1 to 100. As shown in Table 20, when the training epoch number is larger than 5, the learned expert weights by our method are converged on ImageNet-LT, which verifies that our method is robust enough. The corresponding performance on various test class distributions is reported in Table 22.

F.2. Influences of Batch Size

In previous results, we set the batch size of test-time self-supervised aggregation to 128 on all datasets. In this appendix, we further evaluate the influence of the batch size on our strategy, where we adjust the batch size from 64 to 256. As shown in Table 21, with different batch sizes, the learned expert weights by our method keep nearly the same, which shows that our method is insensitive to the batch size. The corresponding performance on various test class distributions is reported in Table 23, where the performance is also nearly the same when using different batch sizes.

Test Dist.	Epoch 1				Epoch 5				Epoch 10			
	Many	Med.	Few	All	Many	Med.	Few	All	Many	Med.	Few	All
Forward-LT-50	68.8	54.6	37.5	68.5	70.0	53.2	33.1	69.4	70.1	52.9	32.4	69.5
Forward-LT-25	68.6	54.9	34.9	66.9	69.5	53.2	32.2	67.4	69.7	52.5	32.5	67.5
Forward-LT-10	60.3	55.3	37.6	65.2	69.9	54.3	34.7	65.4	69.9	54.5	35.0	65.4
Forward-LT-5	68.4	55.3	37.3	63.0	68.9	54.8	35.8	63.0	68.8	54.9	36.0	63.0
Forward-LT-2	67.9	56.2	40.8	60.6	68.2	56.0	40.1	60.6	68.2	56.0	39.7	60.5
Uniform	66.7	56.9	43.1	58.8	66.5	57.0	43.5	58.8	66.4	56.9	43.4	58.8
Backward-LT-2	65.6	57.1	44.7	57.1	65.3	57.1	45.0	57.1	65.3	57.1	45.0	57.1
Backward-LT-5	63.9	57.6	46.8	55.5	63.4	56.4	47.5	55.5	63.3	57.4	47.8	55.6
Backward-LT-10	62.1	57.6	47.9	54.2	60.9	57.5	50.1	54.5	61.1	57.6	48.9	54.5
Backward-LT-25	62.4	57.6	48.5	53.4	60.5	57.1	50.0	53.7	60.5	57.1	50.3	53.8
Backward-LT-50	64.9	56.7	47.8	51.9	60.7	56.2	50.7	53.1	60.1	55.9	51.2	53.2

Test Dist.	Epoch 20				Epoch 50				Epoch 100			
	Many	Med.	Few	All	Many	Med.	Few	All	Many	Med.	Few	All
Forward-LT-50	70.3	52.2	32.4	69.5	70.3	52.2	32.4	69.5	70.0	52.2	32.4	69.3
Forward-LT-25	69.8	52.4	31.4	67.5	69.9	52.3	31.4	67.6	69.7	52.6	32.6	67.5
Forward-LT-10	69.6	54.8	35.8	65.3	69.8	54.6	35.2	65.4	69.8	54.6	35.0	65.4
Forward-LT-5	68.7	55.0	36.4	63.0	68.	55.0	36.4	63.0	68.7	54.7	36.7	62.9
Forward-LT-2	68.1	56.0	39.9	60.5	68.3	55.9	39.6	60.5	68.2	56.0	40.1	60.6
Uniform	66.7	56.9	43.2	58.8	66.9	56.8	42.8	58.8	66.5	56.8	43.2	58.7
Backward-LT-2	65.4	57.1	44.9	57.1	65.6	57.0	44.7	57.1	64.9	57.0	45.6	57.0
Backward-LT-5	63.4	57.4	47.6	55.5	62.7	57.4	48.3	55.6	63.4	57.5	47.0	55.4
Backward-LT-10	60.7	57.5	49.4	54.6	61.1	57.6	48.8	54.4	60.6	57.6	49.1	54.5
Backward-LT-25	60.4	57.1	50.4	53.9	60.4	57.0	50.3	53.8	60.9	56.8	50.2	53.7
Backward-LT-50	60.9	56.1	51.1	53.2	60.6	55.9	51.1	53.2	60.8	56.1	51.2	53.2

Table 22. The influence of the epoch number on the performance of test-time self-supervised aggregation on ImageNet-LT.

Test Dist.	Batch size 64				Batch size 128				Batch size 256			
	Many	Med.	Few	All	Many	Med.	Few	All	Many	Med.	Few	All
Forward-LT-50	70.0	52.6	33.8	69.3	70.0	53.2	33.1	69.4	69.7	53.8	34.6	69.2
Forward-LT-25	69.6	53.0	33.3	67.5	69.5	53.2	32.2	67.4	69.2	53.7	32.8	67.2
Forward-LT-10	69.9	54.3	34.8	65.4	69.9	54.3	34.7	65.4	69.5	55.0	35.9	65.3
Forward-LT-5	69.0	54.6	35.6	63.0	68.9	54.8	35.8	63.0	68.8	54.9	36.0	63.0
Forward-LT-2	68.2	56.0	40.0	60.6	68.2	56.0	40.1	60.6	68.1	56.0	40.1	60.5
Uniform	66.9	56.6	42.4	58.8	66.5	57.0	43.5	58.8	66.5	56.9	43.3	58.8
Backward-LT-2	64.9	57.0	45.7	57.0	65.3	57.1	45.0	57.1	65.5	57.1	44.8	57.1
Backward-LT-5	63.1	57.4	47.3	55.4	63.4	56.4	47.5	55.5	63.4	56.4	47.5	55.5
Backward-LT-10	60.9	57.7	48.6	54.4	60.9	57.5	50.1	54.5	61.3	57.6	48.7	54.4
Backward-LT-25	60.8	56.7	50.1	53.6	60.5	57.1	50.0	53.7	61.0	57.2	49.6	53.6
Backward-LT-50	61.1	56.2	50.8	53.1	60.7	56.2	50.7	53.1	61.2	56.4	50.0	52.9

Table 23. The influence of the batch size on the performance of test-time self-supervised aggregation on ImageNet-LT.

Test Dist.	Learning rate 0.001			Learning rate 0.01			Learning rate 0.025		
	E1 (w_1)	E2 (w_2)	E3 (w_3)	E1 (w_1)	E2 (w_2)	E3 (w_3)	E1 (w_1)	E2 (w_2)	E3 (w_3)
Forward-LT-50	0.36	0.34	0.30	0.49	0.33	0.18	0.52	0.35	0.13
Forward-LT-25	0.36	0.34	0.30	0.48	0.34	0.18	0.50	0.35	0.15
Forward-LT-10	0.36	0.34	0.30	0.45	0.34	0.21	0.46	0.36	0.18
Forward-LT-5	0.36	0.33	0.31	0.43	0.34	0.23	0.43	0.34	0.23
Forward-LT-2	0.35	0.33	0.32	0.38	0.33	0.29	0.37	0.35	0.28
Uniform	0.33	0.33	0.34	0.34	0.33	0.33	0.33	0.33	0.34
Backward-LT-2	0.32	0.32	0.36	0.30	0.32	0.38	0.29	0.31	0.40
Backward-LT-5	0.31	0.32	0.37	0.25	0.31	0.44	0.24	0.31	0.45
Backward-LT-10	0.31	0.32	0.37	0.22	0.29	0.49	0.21	0.29	0.50
Backward-LT-25	0.31	0.32	0.37	0.21	0.28	0.51	0.18	0.29	0.53
Backward-LT-50	0.31	0.32	0.37	0.20	0.28	0.52	0.17	0.27	0.56

Test Dist.	Learning rate 0.05			Learning rate 0.1			Learning rate 0.5		
	E1 (w_1)	E2 (w_2)	E3 (w_3)	E1 (w_1)	E2 (w_2)	E3 (w_3)	E1 (w_1)	E2 (w_2)	E3 (w_3)
Forward-LT-50	0.53	0.36	0.11	0.53	0.37	0.10	0.57	0.34	0.09
Forward-LT-25	0.51	0.36	0.13	0.52	0.36	0.12	0.57	0.34	0.09
Forward-LT-10	0.45	0.37	0.18	0.47	0.36	0.18	0.44	0.36	0.20
Forward-LT-5	0.42	0.35	0.23	0.47	0.36	0.18	0.39	0.36	0.25
Forward-LT-2	0.38	0.24	0.28	0.42	0.36	0.22	0.36	0.34	0.30
Uniform	0.33	0.33	0.34	0.31	0.31	0.38	0.33	0.34	0.33
Backward-LT-2	0.30	0.31	0.39	0.31	0.30	0.39	0.29	0.31	0.40
Backward-LT-5	0.24	0.31	0.45	0.24	0.29	0.47	0.21	0.28	0.51
Backward-LT-10	0.21	0.30	0.49	0.21	0.31	0.48	0.22	0.32	0.46
Backward-LT-25	0.16	0.28	0.56	0.17	0.31	0.52	0.15	0.30	0.55
Backward-LT-50	0.15	0.28	0.57	0.14	0.28	0.58	0.12	0.27	0.61

Table 24. The influence of the learning rate on the learned expert weights by test-time self-supervised aggregation on ImageNet-LT, where the number of the training epoch is 5.

F.3. Influences of Learning Rate

In this appendix, we evaluate the influence of the learning rate on our strategy, where we adjust the learning rate from 0.001 to 0.5. As shown in Table 24, with the increase of the learning rate, the learned expert weights by our method are sharper and fit the unknown test class distributions better. For example, when the learning rate is 0.001, the weight for expert E_1 is 0.36 on the Forward-LT-50 test distribution, while when the learning rate increases to 0.5, the weight for expert E_1 becomes 0.57 on the Forward-LT-50 test distribution. Similar phenomenons can also be observed on backward long-tailed test class distributions.

By observing the corresponding model performance on various test class distributions in Table 25, we find that when the learning rate is too small (e.g., 0.001), our test-time self-supervised aggregation strategy is unable to converge, given a fixed training epoch number 5. In contrast, given the same training epochs, our method can obtain better performance by reasonably increasing the learning rate. Note that, a too-large learning rate may also degenerate the model.

F.4. Results of Prediction Confidence

In our theoretical analysis (i.e., Theorem 1), we find that our test-time self-supervised aggregation strategy not only simulates the test class distribution, but also makes the model predictions more confident. In this appendix, we further evaluate whether our strategy indeed improves the prediction confidence of models on various unknown test class distributions of ImageNet-LT. Therefore, we compare the prediction confidence of our method without and with test-time self-supervised aggregation in terms of the hard mean of the highest prediction probability on all test samples.

As shown in Table 26, our test-time self-supervised aggregation strategy enables the deep model to have higher prediction confidence. For example, on the Forward-LT-50 test distribution, our strategy obtains 0.015 confidence improvement, which is non-trivial since it is an average value for a large number of samples (more than 10,000 samples). In addition, when the class imbalance ratio becomes larger, our method is able to obtain more significant confidence improvement.

Test Dist.	Learning rate 0.001				Learning rate 0.01				Learning rate 0.025			
	Many	Med.	Few	All	Many	Med.	Few	All	Many	Med.	Few	All
Forward-LT-50	67.3	56.1	44.1	67.3	69.5	54.0	34.6	69.0	70.0	53.2	33.1	69.4
Forward-LT-25	67.4	56.2	40.3	66.1	69.2	53.8	33.2	67.2	69.5	53.2	32.2	67.4
Forward-LT-10	67.7	56.4	41.9	64.5	69.6	55.0	36.1	65.4	69.9	54.3	34.7	65.4
Forward-LT-5	67.2	55.9	40.8	62.6	68.7	55.0	36.2	63.0	68.9	54.8	35.8	63.0
Forward-LT-2	67.5	56.2	41.7	60.5	68.1	56.0	40.1	60.5	68.2	56.0	40.1	60.6
Uniform	66.9	56.6	42.7	58.8	67.0	56.8	42.7	58.8	66.5	57.0	43.5	58.8
Backward-LT-2	66.5	56.8	43.3	56.9	65.5	57.1	44.8	57.1	65.3	57.1	45.0	57.1
Backward-LT-5	65.8	57.5	43.7	55.0	63.9	57.5	46.9	55.5	63.4	56.4	47.5	55.5
Backward-LT-10	64.6	57.5	43.7	53.1	61.3	57.6	48.6	54.4	60.9	57.5	50.1	54.5
Backward-LT-25	66.0	57.3	44.1	51.5	61.1	57.4	49.3	53.5	60.5	57.1	50.0	53.7
Backward-LT-50	68.2	56.8	43.7	50.0	63.1	56.5	49.5	52.7	60.7	56.2	50.7	53.1

Test Dist.	Learning rate 0.05				Learning rate 0.1				Learning rate 0.5			
	Many	Med.	Few	All	Many	Med.	Few	All	Many	Med.	Few	All
Forward-LT-50	70.2	52.4	32.4	69.5	70.3	52.3	32.4	69.5	70.3	51.2	32.4	69.5
Forward-LT-25	69.7	52.5	32.5	67.5	69.9	52.3	31.4	67.6	69.9	51.1	29.5	67.5
Forward-LT-10	69.7	54.7	35.8	65.4	69.9	54.3	34.8	65.4	69.5	55.0	35.8	65.3
Forward-LT-5	68.8	54.9	36.2	63.0	68.8	54.8	36.1	63.0	68.3	55.3	37.6	62.9
Forward-LT-2	68.3	56.0	39.6	60.5	68.0	56.1	40.2	60.5	67.1	56.5	42.3	60.5
Uniform	66.6	56.9	43.2	58.8	65.6	57.1	44.7	58.7	67.8	56.4	40.9	58.7
Backward-LT-2	65.4	57.1	44.9	57.1	65.6	57.0	44.5	57.0	65.3	57.1	45.2	57.1
Backward-LT-5	63.6	57.5	48.9	55.4	63.0	57.4	48.1	55.6	61.4	57.4	49.2	55.6
Backward-LT-10	61.1	57.5	48.9	54.4	61.3	57.6	48.6	54.4	62.0	57.5	47.9	54.2
Backward-LT-25	59.9	56.8	51.0	53.9	60.9	57.2	49.9	53.7	60.2	56.8	50.8	53.9
Backward-LT-50	60.1	56.0	51.2	53.2	59.6	55.8	51.3	53.2	58.2	55.6	52.2	53.5

Table 25. The influence of learning rates on test-time self-supervised aggregation on ImageNet-LT, under training epoch 5.

Method	Prediction confidence on ImageNet-LT										
	Forward-LT					Uniform	Backward-LT				
	50	25	10	5	2	1	2	5	10	25	50
Ours w/o test-time aggregation	0.694	0.687	0.678	0.665	0.651	0.639	0.627	0.608	0.596	0.583	0.574
Ours w test-time aggregation	0.711	0.704	0.689	0.674	0.654	0.639	0.625	0.609	0.599	0.589	0.583

Table 26. Comparison of prediction confidence between our method without and with test-time self-supervised aggregation on ImageNet-LT, in terms of the hard mean of the highest prediction probability on each sample. The higher of the highest prediction, the better of the model.

F.5. Run-time Cost of Test-time Aggregation

One may be interested in the run-time cost of our test-time self-supervised aggregation strategy, so we further report its running time on Forward-LT-50 and Forward-LT-25 test class distributions for illustration. As shown in Table 27, our test-time self-supervised aggregation strategy is fast in terms of per-epoch time. The result is easy to interpret since we freeze the model parameters and only learn the aggregation weights, which is much more efficient than the training of the whole model. More importantly, the goal of this paper is to handle a new and practical test-agnostic long-tailed recognition task. For solving this challenging problem, it is acceptable to allow models to be trained more, while promising results in

Dataset	Model training	Test-time weight learning	
		Forward-LT-50	Forward-LT-25
Per-epoch time	713 s	110 s	130 s

Table 27. Run-time cost of our test-time self-supervised aggregation strategy on ImageNet-LT, compared to the run-time cost of model training. Here, we show two test class distributions for illustration, which have different numbers of test samples.

previous experiments have demonstrated the effectiveness of the proposed test-time self-supervised learning strategy in handling this problem.

ImageNet-LT (ResNeXt-50)													
Method	Params (M)	MACs (G)	Forward-LT					Uniform	Backward-LT				
			50	25	10	5	2	1	2	5	10	25	50
Softmax	25.03 (1.0x)	4.26 (1.0x)	66.1	63.8	60.3	56.6	52.0	48.0	43.9	38.6	34.9	30.9	27.6
RIDE [41]	38.28 (1.5x)	6.08 (1.4x)	67.6	66.3	64.0	61.7	58.9	56.3	54.0	51.0	48.7	46.2	44.0
TADE (ours)	38.28 (1.5x)	6.08 (1.4x)	69.4	67.4	65.4	63.0	60.6	58.8	57.1	55.5	54.5	53.7	53.1

CIFAR100-LT-IR100 (ResNet-32)													
Method	Params (M)	MACs (G)	Forward-LT					Uniform	Backward-LT				
			50	25	10	5	2	1	2	5	10	25	50
Softmax	0.46 (1.0x)	0.07 (1.0x)	63.3	62.0	56.2	52.5	46.4	41.4	36.5	30.5	25.8	21.7	17.5
RIDE [41]	0.77 (1.5x)	0.10 (1.4x)	63.0	59.9	57.0	53.6	49.4	48.0	42.5	38.1	35.4	31.6	29.2
TADE (ours)	0.77 (1.5x)	0.10 (1.4x)	65.9	62.5	58.3	54.8	51.1	49.8	46.2	44.7	43.9	42.5	42.4

Places-LT (ResNet-152)													
Method	Params (M)	MACs (G)	Forward-LT					Uniform	Backward-LT				
			50	25	10	5	2	1	2	5	10	25	50
Softmax	60.19 (1.0x)	11.56 (1.0x)	45.6	42.7	40.2	38.0	34.1	31.4	28.4	25.4	23.4	20.8	19.4
RIDE [41]	88.07 (1.5x)	13.18 (1.1x)	43.1	41.8	41.6	42.0	41.0	40.3	39.6	38.7	38.2	37.0	36.9
TADE (ours)	88.07 (1.5x)	13.18 (1.1x)	46.4	44.9	43.3	42.6	41.3	40.9	40.6	41.1	41.4	42.0	41.6

iNaturalist 2018 (ResNet-50)													
Method	Params (M)	MACs (G)	Forward-LT				Uniform	Backward-LT					
			3		2		1	2		3			
Softmax	25.56 (1.0x)	4.14 (1.0x)	65.4		65.5		64.7	64.0		63.4			
RIDE [41]	39.07 (1.5x)	5.80 (1.4x)	71.5		71.9		71.8	71.9		71.8			
TADE (ours)	39.07 (1.5x)	5.80 (1.4x)	72.3		72.5		72.9	73.5		73.3			

Table 28. Model complexity and performance of different methods in terms of the parameter number, Multiply–Accumulate Operations (MACs) and top-1 accuracy on test-agnostic long-tailed recognition. Here, we do not use the efficient expert assignment trick in [41] for RIDE and our method.

G. More Discussions on Model Complexity

In this appendix, we discuss the model complexity of our method in terms of the number of parameters, multiply-accumulate operations (MACs) and top-1 accuracy on test-agnostic long-tailed recognition.

As shown in Table 28, both TADE and RIDE belong to ensemble learning based long-tailed learning methods, so they have more parameters (about 1.5x) and MACs (about 1.4x) than the original backbone model, where we do not use the efficient expert assignment trick in [41] for both methods. Because of the ensemble effectiveness of the multi-expert scheme, both methods perform much better than non-ensemble methods (*e.g.*, Softmax and other long-tailed methods). In addition, since our method and RIDE use the same multi-expert framework, both methods have the same number of parameters and MACs. Nevertheless, by using our proposed skill-diverse expert learning and test-time self-supervised aggregation strategies, our method performs much better than RIDE with no increase in model parameters and computational costs.

One may concern the multi-expert scheme leads to more model parameters and higher computational costs. However, note that the main focus of this paper is to solve challenging test-agnostic long-tailed recognition, while promising results have shown that our method addresses this problem well. In this sense, slightly increasing the model complexity is acceptable for solving this practical and challenging problem. Moreover, since there have already been many studies [16, 42] showing effectiveness in improving the efficiency of the multi-expert scheme, we think the computation increment is not a severe issue and we leave it to the future.